Research Square

Preprints are preliminary reports that have not undergone peer review.
They should not be considered conclusive, used to inform clinical practice,
or referenced by the media as validated information.

Ex Vitro Physiological, Antioxidant and Metabolomic Responses of Salt-Tolerant Salicornia lagascae Clones Derived from Solid and Liquid Micropropagation Systems

Ghofrane Atrous
Center of Biotechnogy of Borj Cédria
Pedro Diaz-Vivancos
Centro de Edafología y Biología Aplicada del Segura
Abel Piqueras
Centro de Edafología y Biología Aplicada del Segura
Ana Hernández-Cánovas
Centro de Edafología y Biología Aplicada del Segura
Gregorio Barba-Espin
Centro de Edafología y Biología Aplicada del Segura
José Antonio Hernández
jahernan@cebas.csic.es
Centro de Edafología y Biología Aplicada del Segura

Research Article

Keywords: Antioxidant metabolism, in vitro selection, photosynthesis, metabolomic profiling, saline agriculture

Posted Date: July 27th, 2026

DOI: https://doi.org/10.21203/rs.3.rs-10392099/v1

License: This work is licensed under a Creative Commons Attribution 4.0 International License. Read Full License

Additional Declarations: No competing interests reported.

Abstract

Halophytes are increasingly recognized for their salt-tolerance and their potential in soil restoration and saline agriculture. However, studies optimizing *in vitro* propagation and evaluating *ex vitro* performance to improve post-transplant growth and propagation efficiency remain scarce. This study demonstrates the effectiveness of *in vitro* techniques for selecting and propagating elite clones of *Salicornia lagascae* with enhanced salinity tolerance. Plants micropropagated in solid and liquid culture systems (S and L plants, respectively) were acclimated *ex vitro* and subsequently exposed to 30 (S30 and L30) or 60 (S60 and L60) g L^{-1} NaCl for six weeks. Electrical conductivity was higher in shoots than in roots and substrate, indicating strong ion accumulation in aerial tissues, correlating with Na^+ and Cl^- levels. L plants generally exhibited greater photosynthetic efficiency and enhanced non-photochemical energy dissipation under stress over time, while lower salinity promoted higher electron transport rates. High salinity decreased APX activity, while CAT, SOD, and POX activities were maintained, indicating effective oxidative stress control under severe salinity. Metabolomic analysis revealed strong separation of S30 plants, showing the greatest metabolic reprogramming, including activation of amino acid, carbohydrate, flavonoid, terpenoid, and stress-related secondary metabolic pathways. In contrast, plants exposed to 60 g L^{-1} NaCl likely redirected energy toward survival and ion homeostasis, with more limited metabolic adjustments. Likewise, L plants exhibited more homogeneous metabolomic profiles, likely because liquid micropropagation enhanced physiological acclimation and reduced the need for large-scale metabolic reprogramming after transplantation. Overall, the remarkable salt tolerance of *S. lagascae* is supported by the coordinated action of ion homeostasis, photoprotective mechanisms, antioxidant defenses, and metabolic reprogramming. Results demonstrate that *in vitro* selection and micropropagation constitute efficient strategies for generating elite halophytic germplasm suitable for saline agriculture, phytoremediation, and soil restoration programs.

1. Introduction

According to the Global Salt-Affected Soils Map, released by the Food and Agriculture Organization (FAO 2024), about 1,400 million hectares of soil worldwide are currently affected by salinity, representing around 10% of the global land area. Moreover, rising salinity levels are causing approximately 1.5 million hectares of agricultural land to become unsuitable for cultivation each year, posing a significant threat to global food security. Consequently, it is anticipated that by the mid-21st century, up to 50% of all cultivable land may be affected by salinity (FAO 2021).

Traditional approaches to managing salinity—such as soil leaching, chemical amendments, or breeding for salt tolerance—are often costly, slow to implement, or limited in effectiveness under severe conditions. Consequently, ecological intensification strategies are gaining increasing attention as sustainable alternatives for restoring soil health and maintaining productivity in salt-affected agroecosystems (Pretty et al. 2018). Among these, agricultural managing systems that incorporate halophytic plants – *i.e.*, intercropping and crop rotation – represent a promising and innovative approach. Halophytic plants are defined as plant species that inhabit saline environments, comprising about 1% of the world´s flora. They are specifically adapted to complete their life cycle in conditions where the salt concentration, mainly in the form of NaCl, reaches or exceeds 200 mM (Flower and Colmer 2008). There is a growing body of research showing that halophytic plants significantly influence crop performance under saline conditions (Karakas et al. 2021; Jurado-Mañogil et al. 2023; Jurado et al. 2024; Slatni et al. 2024; Vicente et al. 2024).

Research on the tissue culture of halophytes has expanded considerably in recent years, addressing objectives such as the conservation and propagation of threatened species, enhancement of bioactive metabolite production, and large-scale multiplication of plants with restricted sexual or vegetative reproduction capabilities (Custodio et al. 2023; Gulzar et al. 2020). In halophytic species, this approach has been extensively applied to produce clonal lines selected for improved salt tolerance (Jurado-Mañogil et al. 2024; de Jesus Raposo et al. 2021; Yao et al. 2021; Vyas et al. 2011). Despite these advances, studies integrating the micropropagation of halophyte clones with subsequent *ex vitro* assessment for potential agricultural and breeding applications remain limited. Agar, because of its chemically inert properties, which minimize interactions with plant metabolic processes, is the gelling agent most frequently employed in *in vitro* culture systems (Ozel et al. 2008). Nevertheless, its application has also been linked to negative impacts on the growth and differentiation of cultured tissues (Mbiyu et al. 2012). In this regard, several studies report that liquid media (flasks, temporary immersion systems and liquid bioreactors) can outperform solid/agar media for shoot proliferation, biomass accumulation, rooting, or overall growth during micropropagation (Liu et al. 2004; Zheleznichenko et al. 2024). Moreover, plants derived from liquid media may be established more vigorously under *ex vitro* conditions (Adelberg et al., 2000; Atrous et al. 2026).

In our earlier research, the *in vitro* performance of highly salt-tolerant clones of the halophyte *Salicornia lagascae* was compared on solid and liquid media. Liquid culture conferred enhanced micronutrient accumulation, improved rhizogenesis, and greater plant

growth after acclimatization, supporting their potential for efficient micropropagation (Atrous et al. 2025). Building upon these findings, the present study investigates whether micropropagation of the halophyte *S. lagascae* in liquid medium enhances *ex vitro* plant performance compared with propagation on solid medium. A comprehensive physiological and biochemical assessment was conducted under greenhouse conditions at different salinity levels. To the best of our knowledge, this is the first study to provide an *ex vitro* comparative characterization of halophyte clones derived from liquid- and solid-based micropropagation systems, emphasizing the importance of optimizing culture methods to improve post-transplant growth and commercial propagation efficiency.

2. Material and Methods

2.1. Plant Material and Experimental Setup

A clonal *S. lagascae* line tolerant to 30 g L^{-1} NaCl was micropropagated either in solid or liquid media, rooted and acclimated to *ex vitro* conditions, as previously described (Atrous et al. 2026). Acclimatized plants were transplanted into 4-L pots containing a peat:perlite mixture (80:20, *v/v*). The experiment was conducted in the glasshouse facilities of the University of Murcia (Espinardo, Region of Murcia, Spain). Prior to treatment application, plants were lightly pruned to obtain uniform size and morphology and allowed to acclimate to greenhouse conditions for one week. During this week, plants were irrigated with Hoagland's solution containing 30 g L^{-1} NaCl. Subsequently, plants derived from micropropagation on solid medium (S plants) and in liquid medium (L plants) were irrigated once per week with 450 mL of Hoagland's solution containing either 30 g L^{-1} NaCl (S30 and L30 plants) or 60 g L^{-1} NaCl (S60 and L60 plants) for 6 weeks. Relative humidity was maintained at approximately 60%, while temperatures ranged from 18°C at night to 34°C during the day, with an average daily temperature of 25°C, simulating natural environmental fluctuations.

2.2. Mineral Nutrients and Electrical Conductivity Monitoring

Macro- and micronutrients were analysed at the end of the assay in shoots and roots samples, as well as in the substrate. Substrate samples were dried at room temperature. Plant samples were thoroughly washed with tap water followed by distilled water. Afterwards, the samples were oven-dried at 70 °C for four days. After drying, samples were ground and filtered through a sieve. For macro- and micro-nutrient analysis, samples were digested using HNO_3/H_2O_2 (4/1, *v/v*) in a high-performance microwave digestion system (Ultraclave; Milestone, Shelton, CT, USA), followed by determination using inductively coupled plasma-optical emission spectrometry (ICP-OES) (ICAP 6000SERIES spectrometer, Thermo Scientific, Madrid, Spain). For anion analysis, dried material was extracted in distilled water (1/10, *w/v* for shoots; 1/15, *w/v* for roots and substrate), heated at 75° C for 3 h and incubated for 24 h at room temperature in continuous agitation. Subsequently, samples were centrifuged at 4000 rpm (Allegra X-22, Beckman Coulter, Inc, Brea, CA, USA) in a swinging bucket rotor for 10 min and the supernatants were filtered through 0.45 µm Minisart filters (Sartorius, Goettingen, Germany). Anions were determined by ion-chromatography (Metrohm Ltd., Herisau, Switzerland). The same aqueous solutions were used to monitor electrical conductivity (EC) using a conductometer (Eutech Instruments CON 150, Singapore).

2.3. Chlorophyll fluorescence determination

Chlorophyll fluorescence was measured with a chlorophyll fluorimeter (IMAGIM-PAM M-series, HeinzWalz, Eeltrich, Germany) over the evolution of the experiment at 0, 7, 14, 28 and 42 days of the initiation of the saline treatments in each type of plants. In brief, after a dark incubation period (20 min), the minimum and the maximal fluorescence yields of the *S. lagascae* shoots were monitored. Kinetic analyses were carried out with actinic light (81 µmol quanta m^{-2} s^{-1} PAR) and repeated pulses of saturating light at 2700 µmol quanta m^{-2} s^{-1} PAR for 0.8 s, and at intervals of 20 s (Atrous et al. 2026; Acosta-Motos et al. 2019). The following parameters were analysed: the maximal PSII quantum yield (Fv/Fm), effective PSII quantum yield [Y(II)], the non-photochemical quenching (NPQ), the coefficients of non-photochemical quenching and photochemical quenching (qN and qP, respectively) and electro transport rate (ETR).

2.4. Antioxidant metabolism

2.4.1. Lipid Peroxidation

Lipid peroxidation levels were evaluated at the end of the experimental period in *S. lagascae* shoots through the quantification of thiobarbituric acid-reactive substances (TBARS), in accordance with the procedures established by Acosta-Motos et al. (2019).

2.4.2. Enzymes Extraction and Analysis

At the end of the experimental period, shoots of *S. lagascae* plants (about 0.5 g) were snap-frozen in liquid nitrogen and preserved at − 80°C until further analysis. Samples were ground with liquid nitrogen and extracted (1/5, *w/v*) in ice-cooled extraction buffer (50 mM Tris-acetate, pH 6.0) supplemented with 0.1 mM EDTA, 2 mM cysteine, 0.2% (*v/v*) Triton X-100, 2% polyvinylpyrrolidone (*w/v*) and 2% polyvinylpolypyrrolidone (*w/v*). For ascorbate peroxidase (APX) activity, 20 mM sodium ascorbate was added to the extraction buffer. The extracts were centrifuged at 12000 *g* for 15 min at 4° C. The supernatant fractions were filtered on Sephadex NAP-10 columns (GE Healthcare, Chicago, IL, USA) equilibrated with 50 mM Tris-acetate buffer (pH 6.0). For APX activity, additional columns were equilibrated with Tris-acetate buffer containing 2 mM ascorbic acid. APX (EC 1.11.1.11), monodehydroascorbate reductase (MDHAR, EC 1.6.5.4), dehydroascorbate reductase (DHAR, EC 1.8.5.1), glutathione reductase (GR, EC 1.6.4.2), superoxide dismutase (SOD, EC 1.15.1.1), catalase (CAT, EC 1.11.1.6) and peroxidase activities (POX, EC 1.11.1.7) were analyzed following routine protocols described in our laboratory (Hernández et al. 2021a, 2021b; Jurado et al. 2024).

Non-denaturing 10% polyacrylamide gel electrophoresis (PAGE) was performed to separate SOD and POX isozymes using a Mini-Protean II dual slab cell (Bio-Rad, Hercules, CA). SOD isozymes were visualized according to the photochemical method of Weissiger and Fridovich (1973), and their identities were confirmed by selective inhibition with KCN or H_2O_2 (Hernández et al. 1999). The identification of POX isoenzymes was carried out by gel staining with 4-methoxy-α-naphtol for 1 h at 25°C in the presence of 50 mm Tris-acetate buffer (pH 5.0) and 0.5 mm H_2O_2 (Ros Barceló 1998).

2.5. Metabolomic Approach and Data Analysis

Extraction of root and shoot samples was done with 50% methanol (1/3, *w/v*) and non-targeted metabolomics analyses (by an ultra-performance liquid chromatography–quadrupole-time-of-flight mass spectrometry) were performed as described (Jurado-Mañogil et al. 2023; Barba-Espín et al. 2024).

Metabolomics data were processed using the MetaboAnalyst 5.0 software (https://www.metaboanalyst.ca), with data normalization achieved through logarithmic (base 10) transformation and Pareto scaling. Partial Least-Squares Discriminant Analysis (PLS-DA), and clustering dendrogram analysis were performed to assess sample grouping. Heatmap analysis of the top 25 most variable features (m/z) and volcano plot analysis (fold change ≥ 4, $p \leq 0.05$) were done to visualize differential metabolite profiles. Selected features (m/z) were putatively identified based on accurate mass and MS/MS fragmentation similarity [Human Metabolome database (http://www.hmdb.ca/)]; annotations were assigned at Metabolomics Standards Initiative (MSI) Level 2. A pathway analysis was finally performed based on the Mummichog algorithm (Li et al., 2013). This method enables the identification of significantly altered metabolic pathways by mapping m/z onto curated metabolic network databases through pairwise comparisons. In this analysis, metabolite annotation relied exclusively on accurate mass measurements; consequently, compound identification was assigned at MSI Level 4. For the analysis, primary ion forms were specified, a mass tolerance of 5 ppm was applied, and pathway mapping was conducted against the Kyoto Encyclopedia of Genes and Genomes (KEGG) database using Arabidopsis thaliana as the reference organism (Jurado-Mañogil et al. 2023; Barba-Espín et al. 2024).

3. Results

3.1. Plant performance and Stress Symptoms

After 42 days of irrigation with NaCl under greenhouse conditions, no major differences in overall plant growth were observed between plants treated with 30 g L^{-1} and 60 g L^{-1} NaCl. However, L plants exhibited greater shoot development than S plants under both salinity treatments (Supplementary Fig. S1). Although *S. lagascae* plants tolerated irrigation with 60 g L^{-1} NaCl, after 6 weeks of salinity treatment both plant types showed visible stress symptoms at 60 g L^{-1} NaCl, including chlorosis, partial shoots desiccation, and reddish-brown pigmentation (Supplementary Fig. S1).

3.2. Ion Homeostasis

The plant type (S *vs*. L) did not have a major impact on nutrient concentrations, with the exception of K^+ concentration, which was higher in S plants than in L plants; and of Na^+ levels, which

were higher (13%) in shoots of S30 with respect to L30, but not in S60 compared to L60. (Tables 1 and 2). In contrast, salinity level, as expected, caused a marked variation in most of the macronutrients and anions analyzed. In this regard, higher salinity decreased Ca^{2+}, K^+ and S levels in both shoots and roots, while increased Na^+ concentration in L roots (31% increase in L60 compared to L30) (Table 1;

Supplementary Table S1). In roots, higher salinity decreased Ca^{2+} concentration in both S and L plants, whereas K^+ diminished solely in S plants. In addition, Na^+/K^+ and Na^+/Ca^{2+} ratios in both plant organs increased, especially in L plants (Fig. 1).

Table 1

Effect of NaCl on the macronutrient contents (g/Kg dry weight) in shoots and roots from acclimated *Salicornia lagascae* plants rooted in solid (S) or liquid (L) media, and in soil. Acclimated plants were treated with 30 g/L NaCl during 7 days. Then, half of the plants from each solid or liquid media were treated with 30 g L^{-1} NaCl or 60 g L^{-1} NaCl respectively during 6 weeks. For more information, please consult Fig. 1. Data represent the mean values ± SE of at least 6 different biological samples. Different letters indicate significant differences according the Tukey's Multiple Range Test ($p \leq 0.05$). S-30: acclimated plants from solid media treated with 30 g/l NaCl; S-60 acclimated plants from solid media treated with 60 g/l NaCl. L-30: acclimated plants from liquid media treated with 30 g/l NaCl; L-60 acclimated plants from liquid media treated with 60 g/l NaCl

		Ca	K	Mg	Na	P	S
Shoot	S30	5.35 ± 0.15a	16.2 ± 0.7a	1.49 ± 0.09a	102 ± 2a	2.78 ± 0.27a	3.07 ± 0.14a
	S60	4.64 ± 0.23ab	12.2 ± 0.5b	1.31 ± 0.07ab	98.0 ± 1.9ab	2.07 ± 0.16ab	2.57 ± 0.12b
	L30	5.42 ± 0.30a	15.2 ± 0.2a	1.45 ± 0.02ab	91.1 ± 2.8b	2.69 ± 0.25ab	2.86 ± 0.12ab
	L60	4.23 ± 0.15b	9.9 ± 0.5c	1.23 ± 0.04b	93.8 ± 2.8ab	1.91 ± 0.13b	2.51 ± 0.10b
Root	S30	88.1 ± 4.0a	115 ± 3a	33.1 ± 1.1	15.2 ± 0.6b	41.2 ± 1.3a	22.1 ± 0.9
	S60	65.9 ± 5.0b	92.3 ± 0.7b	28.6 ± 1.1	17.5 ± 1.2ab	35.8 ± 0.5b	20.3 ± 0.3
	L30	85.7 ± 2.2a	95.1 ± 2.5b	32.2 ± 0.4	15.7 ± 1.0b	37.9 ± 1.2ab	21.4 ± 0.4
	L60	67.5 ± 2.1b	89.3 ± 5.9b	30.1 ± 1.8	20.6 ± 0.7a	34.9 ± 0.8b	20.1 ± 0.3
Soil	S30	14.3 ± 0.2a	1.98 ± 0.07ab	1.89 ± 0.04a	61.5 ± 3.9b	0.54 ± 0.02a	2.18 ± 0.05
	S60	10.5 ± 0.3b	1.90 ± 0.07b	1.53 ± 0.04b	92.6 ± 3.9a	0.42 ± 0.01b	2.05 ± 0.05
	L30	14.0 ± 0.4a	2.23 ± 0.04b	1.84 ± 0.08a	67.7 ± 3.8b	0.58±.0.02a	2.31 ± 0.04
	L60	9.9 ± 0.3b	1.74 ± 0.09b	1.41 ± 0.04b	82.1 ± 4.0a	0.43 ± 0.02b	2.16 ± 0.17

Table 2
Effect of NaCl on the main anion contents (g/L) in shoots and roots from acclimated *Salicornia lagascae* plants rooted in solid (S) or liquid (L) media, and in soil. Acclimated plants were treated with 30 g/L NaCl during 7 days. Then, half of the plants from each solid or liquid media were treated with 30 g/L NaCl or 60 g/L NaCl respectively during 6 weeks. For more information, please consult Fig. 1.

		Cl^-	NO_3^-	PO_4^{2-}	SO_4^{2-}
Shoot	**S30**	125 ± 5	5.55 ± 0.31a	9.32 ± 0.69a	29.3 ± 1.5a
	S60	146 ± 3	3.82 ± 0.19b	7.73 ± 0.20b	27.6 ± 0.6b
	L30	136 ± 8	5.30 ± 0.21a	9.10 ± 0.28ab	28.2 ± 1.3ab
	L60	133 ± 8	3.91 ± 0.45b	5.68 ± 0.31c	23.4 ± 1.7b
Root	**S30**	27.0 ± 2.8	0.43 ± 0.01	10.2 ± 0.7a	2.93 ± 0.27
	S60	24.0 ± 3.3	0.42 ± 0.01	7.58 ± 0.35b	2.48 ± 0.26
	L30	24.3 ± 2.0	0.42 ± 0.01	7.66 ± 0.27b	2.59 ± 1.97
	L60	28.0 ± 1.7	0.44 ± 0.02	6.29 ± 0.49b	2.38 ± 0.05
Soil	**S30**	61.5 ± 3.9c	2.18 ± 0.09ab	0.87 ± 0.01a	3.24 ± 0.04ab
	S60	92.6 ± 3.9a	1.78 ± 0.16b	0.77 ± 0.02b	2.98 ± 0.08bc
	L30	67.8 ± 3.8bc	2.36 ± 0.12a	0.91 ± 0.02a	3.27 ± 0.06a
	L60	82.1 ± 4.0ab	1.90 ± 0.07b	0.78 ± 0.02b	2.92 ± 0.07c

Data represent the mean values ± SE of at least 6 different biological samples. Different letters indicate significant differences according the Tukey's Multiple Range Test ($p \leq 0.05$). S-30: acclimated plants from solid media treated with 30 g/l NaCl; S-60 acclimated plants from solid media treated with 60 g/l NaCl. L-30: acclimated plants from liquid media treated with 30 g/l NaCl; L-60 acclimated plants from liquid media treated with 60 g/l NaCl.

Regarding soil samples, 60 g L^{-1} NaCl significantly increased Na^+ accumulation, with a 48% rise in substrate from S plants and ca. 20% in substrate from L plants. In contrast, higher salinity reduced Ca^{2+}, Mg^{2+}, and P availability in all cases (Table 1). Concerning anions, Cl^- accumulated in response to higher salinity, whereas NO_3^-, PO_4^{2-}, and SO_4^{2-} decreased (Table 2).

Regarding micronutrients content, the plant type did not induce any significant changes in either. On the other hand, higher salinity declined Mn^{2+} concentration in shoots of L plants. In roots, higher salinity induced a significant decrease in Fe and Zn^{2+} concentrations only in S plants. The higher NaCl treatment also produced a significant decrease in the concentrations of Cu, Mn^{2+}, and Zn^{2+} in the soil of both plant types (Supplementary Table S2).

Concerning EC, it was markedly higher in shoots than in roots and substrate samples, indicating the strong capacity of the aerial tissues of *S. lagascae* to accumulate solutes. Regarding shoot EC values, S plants displayed approximately 5-fold higher values than those observed in roots, whereas L plants had values approximately 4.4-fold higher than S plants (Fig. 2). In this regards, high EC values in shoots were positively correlated with elevated levels of Na^+ and Cl^- (Tables 1 and 2). Shoots of *S. lagascae* accumulated Na^+ up to about 10% of dry weight and Cl^- ions up to 12–14% (Tables 1 and 2).

3.3. Chlorophyll fluorescence

Chlorophyll fluorescence parameters were monitored at 0, 7, 14, 28, and 42 days of the initiation of the saline treatments. Fv/Fm values below 0.8 throughout the experiment (Supplementary Fig. S2) indicated a moderate photosynthetic stress, although only minor variations were observed among treatments. At day 14, L30 plants exhibited the highest Y(PSII), followed by L60 plants, whereas S30 and S60 showed lower values (Fig. 3A). At day 28, Y(PSII) values were similar across treatments, whereas at day 42, L plants again showed higher photosynthetic efficiency than S plants (Fig. 3B). Photochemical quenching (qP) was lowest in S30 plants at 14 and 42 days, while L30 plants showed the highest qP at later stages (Fig. 3B). ETR was reduced by higher salinity, with S30 and L30 plants showing higher values than S60 and L60 at 14 and 28 days. By day 42, ETR values converged among treatments (Fig. 3c). Non-photochemical quenching parameters were similar during the first week. At day 14, S30 plants showed the highest NPQ and qN values. After 42 days, NPQ increased in all treatments, particularly in L plants (Fig. 3D, E).

3.4. Antioxidant Metabolism

After six weeks of saline treatment, the analysis of lipid peroxidation, commonly used as an oxidative stress indicator, showed that 60 g L^{-1} NaCl did not induce oxidative stress compared with the 30 g L^{-1} NaCl treatments (Supplementary Fig. S3), despite the appearance of visible symptoms of salt stress.

ANOVA analysis showed that culture medium (M factor) significantly influenced MDHAR, DHAR and CAT activities, whereas saline treatment (S factor) significantly affected APX, MDHAR and CAT activities. The interaction (M * S) was significant only for MDHAR and CAT activities (Supplementary Table S3).

Irrigation with 60 g L^{-1} NaCl significantly reduced APX activity in both plant types, with decreases of approximately 40% (Fig. 4A). The activity of MDHAR showed clear differences between S and L plants (Fig. 4B). MDHAR activity remained unchanged in S plants, suggesting that high salinity did not affect NADH-dependent ASC recycling capacity in S plants. In contrast, L60 plants showed a 40% decrease in MDHAR activity compared with L30 plants (Fig. 4B). Conversely, DHAR activity was approximately 2.5-fold higher in S30 than in L30 plants and was unaffected by higher salinity (Fig. 4C). Regarding GR activity, no significant changes were observed (Fig. 4D; Supplementary Table S3).

CAT activity was about 2.6-fold higher in S30 plants than in L30 plants; however, it increased dramatically in L60 plants, reaching nearly six-fold greater levels than L30 (Fig. 4E). POX and SOD activities showed no significant changes (Fig. 4F, G; Supplementary Table S3).

Native PAGE allowed the observation of six different POX isoenzymes in S plants and 5 in L plants (Fig. 5A). On the other hand, by using specific inhibitors, four different SOD isoenzymes were detected in *S. lagascae* shoots (Fig. 5B): two Mn-SODs and two Cu/Zn-SODs (Fig. 5B). Higher salinity reduced the intensity of the Cu/Zn-SOD II band in L60 plants (Fig. 5C).

3.5. Metabolome profile

Metabolomics revealed no significant differences in roots by salinity treatments. In shoots, PCA and clustering dendrogram analyses revealed a clear separation of S30 plants from the other treatments (S60, L30 and L60), which were grouped within the same cluster (Supplementary Fig. S4). Therefore, S60, L30, and L60 were subsequently pooled and analysed as a single group for comparison with S30. The top 25 variable mass features displayed by the heatmap analysis were up-regulated in S30 plants compared the pooled group (Fig. S5). Moreover, volcano plot analysis revealed 1,148 differentially expressed features, of which 763 were up-regulated and only two were down-regulated in S30 shoots compared with the pooled treatments (Supplementary Fig. S6A).

L30 and L60 plants exhibited similar metabolomic profiles (Supplementary Fig. S4). However, when comparing S30 and S60 plants, PCA and clustering dendrogram analysis revealed distinct metabolomic profiles, with a clear separation between both treatments (Supplementary Fig. S7). All top 25 variable mass features displayed on the heatmap analysis (Supplementary Fig. S8) were overexpressed in S30. Additionally, volcano plot analysis revealed 1,035 differentially expressed metabolites, of which 100 were up-regulated and only one was down-regulated in S30 shoots compared with S60 shoots (Supplementary Figure S6B).

The different volcano plot analysis performed showed that three metabolites were significantly down-regulated in *S. lagascae* shoots under S30 conditions. These metabolites were putatively identified (by accurate mass matching and MS/MS fragmentation spectra comparison against the Human Metabolome Database; MSI Level 2) as tridec-7-enoic acid (a fatty acid) and N-methyl-4-aminobutyric acid (a γ-aminobutyric acid derivative) in the comparison S30 *vs* pooled treatments, and pyridoxine (vitamin B6) in the specific comparison between S30 and S60 (Table 3).

Table 3
Putative metabolite identification in *in vitro S.lagascae* shoots based on accurate mass and MS/MS fragmentation pattern comparison, using the Human Metabolome Database (HMDB). Comparison established: S30 vs pooled samples; S30 vs S60.

m/z	Putative identification	Molecular formula	Adduct	Error	Subclass	Database
S30 vs pooled samples						
235.166	tridec-7-enoic acid	$C_{13}H_{24}O_2$	M + Na	1	Fatty acid	HMDB
118.087	N-Methyl-4-aminobutyric acid	$C_5H_{11}NO_2$	M + H	5	GABA derivatives	HMDB
S30 vs S60						
152.071	Pyridoxine	$C_8H_{11}NO_3$	M + H-H2O	1	Vitamine B	HMDB

The Mummichog algorithm (Li et al., 2013) enabled the identification of metabolic pathways altered in S30 shoots compared with the other treatments (pooled S60, L30 and L60 treatments) (Fig. 6A and Table 4). All the affected pathways were up-regulated in S30 samples. This approach allowed the identification (annotation based only on accurate mass; MSI Level 4) of metabolites associated with amino acid metabolism, including valine, isoleucine, arginine, proline, and phenylalanine metabolism (29 metabolites), as well as cyanoamino acid metabolism (10 metabolites). Additional significantly altered pathways included steroid metabolism (11 metabolites), galactose metabolism (9 metabolites), butanoate metabolism (9 metabolites), flavone and flavonol biosynthesis (5 metabolites), isoquinoline alkaloid biosynthesis (4 metabolites) and several terpenoid-derived metabolites, including monoterpenoids (5 metabolites) and steroids (11 metabolites) (Fig. 6A, Table 5).

Table 4
The most affected metabolic pathways in *S.lagascae* shoots according to the Mummichog algorithm (metabolite annotation based solely on accurate mass). Comparison: S30 vs pooled samples.

Pathway	Pathway total	Hits	Adduct	KEEG	Compound name	Molecular formula	m.z	Log2(fc)
Valine leucine and isoleucine biosynthesis	22	14	M + H[1+]	C02612	(R)-2-Methylmalate	$C_5H_8O_5$	*149.045*	*9.9*
			M-H2O + H[1+]	C00123	L-Leucine	$C_6H_{13}NO_2$	*114.091*	*9.8*
			M-H2O + H[1+]	C02226	2-Methylmaleate	$C_5H_6O_4$	*113.023*	*9.5*
			M + H[1+]	C06032	D-erythro-3-Methylmalate	$C_5H_8O_5$	*149.045*	*9.9*
			M-H2O + H[1+]	C00188	L-Threonine	$C_4H_9NO_3$	*102.055*	*9.5*
			M-H2O + H[1+]	C00109	2-Oxobutanoate	$C_4H_5O_3$	*85.028*	*8.7*
			M-H2O + H[1+]	C06006	(S)-2-Aceto-2-hydroxybutanoate	$C_6H_{10}O_4$	*129.054*	*9*
			M-H2O + H[1+]	C14463	(R)-3-Hydroxy-3-methyl-2-oxopentanoate	$C_6H_{10}O_4$	*129.054*	*9*
			M + H[1+]	C00407	L-Isoleucine	$C_6H_{13}NO_2$	*132.102*	*7.1*
			M + H[1+]	C06010	(S)-2-Acetolactate	$C_5H_8O_4$	*133.050*	*9.3*
			M + H[1+]	C04181	3-Hydroxy-3-methyl-2-oxobutanoic acid	$C_5H_8O_4$	*133.050*	*7.7*
			M-H2O + H[1+]	C04272	(R)-2.3-Dihydroxy-3-methylbutanoate	$C_5H_9O_4$	*117.054*	*8.5*
			M-H2O + H[1+]	C00141	3-Methyl-2-oxobutanoic acid	C5H8O3	*99.044*	*8.1*
			M-H2O + H[1+]	C00183	L-Valine	C5H11NO2	*100.076*	*7.8*
Butanoate metabolism	17	9	M + H[1+]	C00025	L-Glutamate	C5H9NO4	*148.06*	*6.9*
			M-H2O + H[1+]	C00164	Acetoacetate	$C_4H_6O_3$	*85.028*	*8.7*
			M + H[1+]	C00334	4-Aminobutanoate	C4H9NO2	*104.071*	*7.7*
			M-H2O + H[1+]	C00989	4-Hydroxybutanoic acid	$C_4H_8O_3$	*87.044*	*7.2*
			M-H2O + H[1+]	C00026	2-Oxoglutarate	$C_5H_6O_5$	*119.018*	*8.1*

Pathway	Pathway total	Hits	Adduct	KEEG	Compound name	Molecular formula	m.z	Log2(fc)
			M + H[1+]	C02630	2-Hydroxyglutarate	$C_5H_8O_5$	*149.045*	*7.7*
			M-H2O + H[1+]	C00232	Succinate semialdehyde	C4H6O3	*85.028*	*8.7*
			M-H2O + H[1+]	C00042	Succinate	$C_4H_4O_4$	*101.023*	*8.1*
C5-Branched dibasic acid metabolism	6	5	M-H2O + H[1+]	C02226	2-Methylmaleate	$C_5H_6O_4$	*113.023*	*9.5*
			M + H[1+]	C02612	(R)-2-Methylmalate	$C_5H_8O_5$	*149.045*	*7.7*
			M + H[1+]	C06032	D-erythro-3-Methylmalate	$C_5H_6O_5$	*149.045*	*6.4*
			M-H2O + H[1+]	C0010	2-Oxobutanoate	$C_4H_5O_3$	*85.028*	*8.7*
			M + H[1+]	C06010	(S)-2-Acetolactate	$C_5H_8O_4$	*133.050*	*9.3*
Monoterpenoid biosynthesis	7	5	M-H2O + H[1+	C00843	(-)-Menthone	$C_{10}H_{18}O$	*137.132*	*8.4*
			M-H2O + H[1+]	C11393	(-)-alpha-Terpineol	$C_{10}H_{18}O$	*137.132*	*8.4*
			M + H[1+]	C06074	Myrcene	$C_{10}H_{16}$	*137.132*	*8.4*
			M-H2O + H[1+]	C11389	(+)-Linalool	$C_{10}H_{18}O$	*137.132*	*8.4*
			M-H2O + H[1+]	C09844	1.8-Cineole	$C_{10}H_{18}O$	*137.132*	*8.4*
Cyanoamino acid metabolism	29	10	M-H2O + H[1+]	C00302	Glutamate	$C_5H_8NO_4$	*130.05*	*7.8*
			M + H[1+]	C00561	Mandelonitrile	C_8H_7NO	*134.060*	*8.3*
			M + H[1+]	C00097	L-Cysteine	$C_3H_7NO_2S$	*122.027*	*9*
			M + H[1+]	C00049	L-Aspartate	$C_4H_7NO_4$	*134.050*	*9*
			M + H[1+]	C18796	(2R)-2-Hydroxy-2-methylbutanenitrile	C_5H_9NO	*100.076*	*8.9*
			M + H[1+]	C03742	(S)-4-Hydroxymandelonitrile	$C_8H_7NO_2$	*150.055*	*9.3*
			M + H[1+]	C00079	L-Phenylalanine	$C_9H_{11}NO_2$	*166.087*	*3.3*
			M-H2O + H[1+]	C19712	N-Hydroxy-L-phenylalanine	$C_9H_{11}NO_3$	*164.070*	*7.6*

Pathway	Pathway total	Hits	Adduct	KEEG	Compound name	Molecular formula	m.z	Log2(fc)
			M-H2O + H[1+]	C19715	N.N-Dihydroxy-L-phenylalanine	$C_9H_{11}NO_4$	*180.066*	*6.7*
			M-H2O + H[1+]	C19715	(E)-Phenylacetaldoxime	C8H9NO	*180.066*	*6.7*
Isoquinoline **alkaloid** biosyn**thesis**	6	4	M + H[1+]	C00082	L-Tyrosine	$C_9H_{11}NO_3$	*182.082*	*6.7*
			M-H2O + H[1+]	C00355	3.4-Dihydroxy-L-phenylalanie	$C_9H_{11}NO_4$	*180.066*	*9.2*
			M + H[1+]	C03758	Dopamine	$C_9H_{11}NO_4$	*154.086*	*2.4*
			M-H2O + H[1+]	C04043	3.4-Dihydroxyphenylacetaldehyde	$C_8H_8O_3$	*135.044*	*1*
Arginine and proline metabolism	32	10	M + H[1+]	C00062	L-Arginine	$C_6H_{14}N_4O_2$	*175.119*	*1*
			M + H[1+]	C05936	N4-Acetylaminobutanal	$C_6H_{11}NO_2$	*130.086*	*1*
			M-H2O + H[1+]	C05938	L-4-Hydroxyglutamate semialdehyde	$C_5H_9NO_4$	*130.050*	*7.8*
			M + H[1+]	C04281	L-1-Pyrroline-3-hydroxy-5-carboxylate	$C_5H_6NO_3$	*130.050*	*9.6*
			M + H[1+]	C00148	L-Proline	$C_5H_9NO_2$	*116.071*	*5.1*
			M-H2O + H[1+]	C00019	S-Adenosyl-L-methionine	$C_{15}H_{23}N_6O_5S$	*381.132*	*7.9*
			M + H[1+]	C00750	Spermine	$C_{10}H_{26}N_4$	*203.223*	*9.3*
			M + H[1+]	C00025	L-Glutamate	$C_5H_8NO_4$	*148.06*	*7.8*
			M + H[1+]	C00315	Spermidine	$C_7H_{19}N_3$	*146.165*	*8.9*
			M + H[1+]	C00334	4-Aminobutanoate	$C_4H_9NO_2$	*104.071*	*7.7*
Galactose metabolism	27	9	M + H[1+]	C00243	Lactose	$C_{12}H_{22}O_{11}$	*343.124*	*7.3*
			M + Na[1+]	C05400	Epimelibiose	$C_{12}H_{22}O_{11}$	*365.106*	*7.3*
			M + H[1+]	C00116	Glycerol	$C_3H_8O_3$	*93.055*	*7.8*
			M + Na[1+]	C01613	Stachyose	$C_{24}H_{42}O_{21}$	*689.114*	*8.4*
			M + Na[1+]	C05404	D-Gal alpha 1->6D-Gal alpha 1->6D-Glucose	$C_{18}H_{32}O_{16}$	*527.159*	*9.5*
			M + H[1+]	C01235	alpha-D-Galactosyl-(1->3)-1D-myo-inositol	$C_{12}H_{22}O_{11}$	*343.124*	*7.3*

Pathway	Pathway total	Hits	Adduct	KEEG	Compound name	Molecular formula	m.z	Log2(fc)
			M + Na[1+]	C00492	Raffinose	$C_{18}H_{32}O_{16}$	*527.159*	*9.5*
			M + H[1+]	C05402	Melibiose	$C_{12}H_{22}O_{11}$	*343.124*	*7.3*
			M + Na[1+]	C00089	Sucrose	$C_{12}H_{22}O_{11}$	*365.106*	*7.3*
Flavone and flavonol biosynthesis	10	5	M + H[1+]	C00389	Quercetin	$C_{15}H_{10}O_7$	*303.051*	*6.8*
			M + H[1+]	C12249	Kaempferol 3-O-glucoside	$C_{21}H_{20}O_{11}$	*449.109*	*9.3*
			M + H[1+]	C01750	Quercitrin	$C_{21}H_{20}O_{11}$	*449.109*	*9.3*
			M + H[1+]	C21854	Kaempferol 3-O-rhamnoside-7-O-glucoside	$C_{27}H_{30}O_{15}$	*595.168*	*7.8*
			M + Na[1+]	C19796	Quercetin 3-O-rhamnoside 7-O-glucoside	$C_{27}H_{30}O_{16}$	*633.144*	*7*
Phenylalanine metabolism	12	5	M + H[1+]	C00079	L-Phenylalanine	$C_9H_{11}NO_2$	*166.087*	*3.3*
			M-H2O + H[1+]	C05852	2-Hydroxyphenylacetate	$C_8H_8O_3$	*135.044*	*1*
			M + H[1+]	C02505	2-Phenylacetamide	C_8H_9NO	*136.076*	*2.4*
			M + H[1+]	C07086	Phenylacetic acid	$C_8H_8O_2$	*137.059*	*9.5*
			M + H[1+]	C00601	Phenylacetaldehyde	C_8H_8O	*121.065*	*8.1*
Arachidonic acid metabolism	9	4	M + H[1+]	C02165	Leukotriene B4	$C_{20}H_{32}O$	*337.236*	8.7
			M + H[1+]	C00427	Prostaglandin H2	$C_{20}H_{32}O_5$	*353.231*	*6.9*
			M + H[1+]	C00584	Prostaglandin E2	$C_{20}H_{32}O_5$	*353.231*	*6.9*
			M-H2O + H[1+]	C00639	Prostaglandin F2alpha	$C_{20}H_{34}O_5$	*337.236*	*8.7*
Steroid biosynthesis	44	11	M + Na[1+]	C15782	Delta7-Avenasterol	$C_{29}H_{48}O$	435.360	6.9
			M-H2O + H[1+]	C15783	5-Dehydroavenasterol	$C_{29}H_{46}O$	*393.353*	6.4
			M + Na[1+]	C05442	Stigmasterol	$C_{29}H_{48}O$	*435.360*	6.9
			M-H2O + H[1+]	C11455	4.4-Dimethyl-5alpha-cholesta-8.14.24-trien-3beta-ol	$C_{29}H_{46}O$	*393.353*	6.4
			M + Na[1+]	C05108	14-Demethyl-lanosterol	$C_{29}H_{48}O$	*435.360*	6.9
			M-H2O +	C11508	4alpha-Methyl-5alpha-ergosta-8.14.24(28)-trien-	$C_{29}H_{46}O$	*393.353*	6.4

Pathway	Pathway total	Hits	Adduct	KEEG	Compound name	Molecular formula	m.z	Log2(fc)
			H[1+]		3beta-ol			
			M + Na[1+]	C15776	4alpha-Methylfecosterol	$C_{29}H_{48}O$	*435.360*	6.9
			M + Na[1+]	C11522	24-Methylenelophenol	$C_{29}H_{48}O$	*435.360*	6.9
			M + H[1+]	C22120	4alpha-Carboxy-stigmasta-7.24(24(1))-dien-3beta-ol	$C_{30}H_{48}O_3$	*457.368*	2.9
			M-H2O + H[1+]	C22123	Avenastenone	$C_{29}H_{46}O$	*393.353*	6.4
			M + Na[1+]	C08821	Isofucosterol	$C_{29}H_{48}O$	*435.360*	6.9

Table 5
The most affected metabolic pathways in *S.lagascae* shoots according to the Mummichog algorithm (metabolite annotation based solely on accurate mass). Comparison: S30 vs S60 shoots.

Pathway	Pathway total	Hits	Adduct	KEEG	Compound name	Molecular formula	m.z	Log2(fc)
Butanoate metabolism	17	9	M + H[1+]	C00025	L-Glutamate	C5H9NO4	*148.06*	*6.9*
			M-H2O + H[1+]	C00164	Acetoacetate	$C_4H_6O_3$	*85.028*	*8.7*
			M-H2O + H[1+]	C00026	2-Oxoglutarate	$C_5H_6O_5$	*119.018*	*8.1*
			M + H[1+]	C02630	2-Hydroxyglutarate	$C_5H_8O_5$	*149.045*	*7.7*
			M-H2O + H[1+]	C00232	Succinate semialdehyde	C4H6O3	*85.028*	*8.7*
			M-H2O + H[1+]	C00042	Succinate	$C_4H_4O_4$	*101.023*	*8.1*
C5-Branched dibasic acid metabolism	6	5	M-H2O + H[1+]	C02226	2-Methylmaleate	$C_5H_6O_4$	*113.023*	*9.5*
			M + H[1+]	C02612	(R)-2-Methylmalate	$C_5H_8O_5$	*149.045*	*7.7*
			M + H[1+]	C06032	D-erythro-3-Methylmalate	$C_5H_6O_5$	*149.045*	*6.4*
			M-H2O + H[1+]	C0010	2-Oxobutanoate	$C_4H_5O_3$	*85.028*	*8.7*
			M + H[1+]	C06010	(S)-2-Acetolactate	$C_5H_8O_4$	*133.050*	*9.3*
Monoterpenoid biosynthesis	7	5	M-H2O + H[1+	C00843	(-)-Menthone	$C_{10}H_{18}O$	*137.132*	*8.4*
			M-H2O + H[1+]	C11393	(-)-alpha-Terpineol	$C_{10}H_{18}O$	*137.132*	*8.4*
			M + H[1+]	C06074	Myrcene	$C_{10}H_{16}$	*137.132*	*8.4*
			M-H2O + H[1+]	C11389	(+)-Linalool	$C_{10}H_{18}O$	*137.132*	*8.4*
			M-H2O + H[1+]	C09844	1.8-Cineole	$C_{10}H_{18}O$	*137.132*	*8.4*
Alanine aspartate and glutamate metabolism	22	5	M-H2O + H[1+]	C00026	2-Oxoglutarate	$C_5H_4O_5$	*129.018*	*2.9*
			M-H2O + H[1+]	C00025	L-Glutamate	$C_5H_9NO_4$	*130.050*	*9.6*
			M-H2O + H[1+]	C00232	Succinate semialdehyde	$C_4H_6O_3$	*85.028*	*9.5*
			M-H2O + H[1+]	C00042	Succinate	$C_4H_4O_4$	*101.023*	*8.1*
Arginine and proline metabolism	32	8	M + H[1+]	C00062	L-Arginine	$C_6H_{14}N_4O_2$	*175.119*	*1*
			M + H[1+]	C05936	N4-Acetylaminobutanal	$C_6H_{11}NO_2$	*130.086*	*1*
			M-H2O + H[1+]	C05938	L-4-Hydroxyglutamate semialdehyde	$C_5H_9NO_4$	*130.050*	*7.8*

Pathway	Pathway total	Hits	Adduct	KEEG	Compound name	Molecular formula	m.z	Log2(fc)
			M + H[1+]	C04281	L-1-Pyrroline-3-hydroxy-5-carboxylate	$C_5H_6NO_3$	*130.050*	*9.6*
			M-H2O + H[1+]	C00019	S-Adenosyl-L-methionine	$C_{15}H_{23}N_6O_5S$	*381.132*	*7.9*
			M + H[1+]	C00750	Spermine	$C_{10}H_{26}N_4$	*203.223*	*9.3*
			M + H[1+]	C00025	L-Glutamate	$C_5H_8NO_4$	*148.06*	*7.8*
			M + H[1+]	C00315	Spermidine	$C_7H_{19}N_3$	*146.165*	*8.9*
Galactose metabolism	27	9	M + H[1+]	C00243	Lactose	$C_{12}H_{22}O_{11}$	*343.124*	*7.3*
			M + Na[1+]	C05400	Epimelibiose	$C_{12}H_{22}O_{11}$	*365.106*	*7.3*
			M + H[1+]	C00116	Glycerol	$C_3H_8O_3$	*93.055*	*7.8*
			M + Na[1+]	C01613	Stachyose	$C_{24}H_{42}O_{21}$	*689.114*	*8.4*
			M + Na[1+]	C05404	D-Gal alpha 1->6D-Gal alpha 1->6D-Glucose	$C_{18}H_{32}O_{16}$	*527.159*	*9.5*
			M + H[1+]	C01235	alpha-D-Galactosyl-(1->3)-1D-myo-inositol	$C_{12}H_{22}O_{11}$	*343.124*	*7.3*
			M + Na[1+]	C00492	Raffinose	$C_{18}H_{32}O_{16}$	*527.159*	*9.5*
			M + H[1+]	C05402	Melibiose	$C_{12}H_{22}O_{11}$	*343.124*	*7.3*
			M + Na[1+]	C00089	Sucrose	$C_{12}H_{22}O_{11}$	*365.106*	*7.3*

Comparison of the metabolic responses of S30 and S60 plants by pathway analysis revealed an up-regulation of metabolites associated with amino acid metabolism, including arginine, proline, alanine, aspartate, and glutamate (13 metabolites), as well as C5-branched amino acids (5 metabolites). Other upregulated pathways in S30 included butanoate metabolism (9 metabolites), galactose metabolism (9 metabolites), and monoterpenoid biosynthesis (5 metabolites) (Fig. 6B, Table 5).

4. Discussion

4.1. Overall plant performance and photosynthesis performance

In recent years, halophytic plants have attracted growing interest for their capacity to tolerate high salinity and their potential in soil restoration and saline agriculture (Bazihizina et al., 2024). However, there is a lack of studies that address optimization of *in vitro* cultivation and ulterior characterization *ex vitro* as a way to improve post-transplant growth and commercial propagation efficiency. In this study, *in vitro*-derived *S. lagascae* plants showed high tolerance to irrigation with 60 g L^{-1} NaCl, with minor differences with respect to 30 g L^{-1} NaCl in terms of biomass, photosynthesis efficiency and oxidative stress levels. Plants generally respond to salinity by reducing the rate of photosynthesis, which correlates with plant growth retardation (Wungrampha et al. 2018), and previous studies have reported that *Salicornia* spp. typically show optimal growth at moderate salinity around seawater levels (~ 30–35 g/L NaCl), where biomass production is highest, whereas as salinity increases toward 60 g/L NaCl, plants generally maintain survival but show reduced growth, photosynthetic efficiency, and biomass accumulation (Flowers and Colmer 2008). Thus, our results suggest *in vitro* multiplication and selection of clones as a tool to improve salt tolerance in the *ex vitro* environment. Likewise, the type of

micropropagation (S and L plants) did not have a major impact on plant performance; considering the faster development and multiplication rate of this species in *in vitro* liquid medium (Atrous et al. 2026), this method appears as suitable for mass propagation.

S. lagascae plants exhibited signs of photoinhibition, as reflected by Fv/Fm values below 0.8 (Maxwell and Johnson 2000). However, only slight variations were observed throughout the experiment, indicating that salinity had minimal influence on Fv/Fm during the treatment period. After one week of salt treatments, L30 plants showed higher Y(PSII) and qP values, indicating greater photosynthetic efficiency in plants derived from liquid cultures. The 30 g L^{-1} NaCl treatment also displayed higher ETR, particularly in S plants. On the contrary, higher salinity reduced ETR in the short-term; however, no differences were observed in the long-term, which may indicate a process of acclimatization to the imposed saline conditions. Salt-induced reductions in ETR have previously been associated with photosynthetic impairment in halophytes (Duarte et al. 2013). A differential physiological response was observed between plants subjected to 30 g L^{-1} NaCl and high salinity. S30 plants exhibited the highest short-term ETR values; however, this increase was not associated with enhanced photosynthetic efficiency, as indicated by reduced Y(PSII) and increased NPQ and qN values. This pattern suggests transient photoinhibition together with activation of photoprotective mechanisms to dissipate excess excitation energy, thereby limiting ROS generation (Maxwell and Johnson 2000). In contrast, L30 plants displayed a stronger coupling between elevated ETR and Y(PSII), while maintaining lower NPQ values than S30 plants, indicating a more efficient use of absorbed light energy.

In the long term, all plants showed increased non-photochemical energy dissipation, particularly in L plants, which exhibited the highest NPQ values. These results are consistent with recent findings showing that halophytic species regulate non-photochemical quenching and energy dissipation to preserve photosynthetic performance under high salinity (Shuyskaya et al. 2023; Jordine et al. 2024). A similar response has been reported in *S. europaea*, which exhibited increased Y(NPQ) values after 4–6 weeks of saltwater submergence, suggesting that photoinhibition of photosynthesis functions as an adaptive mechanism to the imposed salinity stress in halophyte plants (Jordine et al. 2024). More recently, Atrous et al. (2025) reported enhanced NPQ parameters in in *vitro*-selected *Arthrocaulon macrostachyum* clones during *ex vitro* acclimation under salinity, correlating with improved plant performance and reduced stress symptoms compared to wild counterparts.

4.2. Ion homeostasis and nutrient imbalance responses

S. lagascae exhibited a remarkable capacity to accumulate toxic ions in shoots, particularly Na^+, Cl^-, and SO_4^{2-}, consistent with EC measurements. Similar results were reported for *A. macrostachyum* plants grown under increasing NaCl concentrations, which accumulated a high concentration of phytotoxic ions in their aerial parts, highlighting their desalting capacity (Jurado-Mañogil et al. 2024; Atrous et al. 2025). This ion accumulation, likely coupled with vacuolar sequestration, contributes to osmotic adjustment by using Na^+ and Cl^- as low-cost osmolytes, thereby facilitating water uptake and helping plants maintain shoot turgor (Shabala and Mackay 2011).

S. lagascae plants accumulated high amounts of Na^+ in shoots; however, this accumulation was not proportional to external salinity, suggesting tight regulation of uptake and compartmentalization mechanisms. This suggests a distinct pattern of Na^+ regulation compared with other Salicornia species, in which Na^+ levels in shoots and roots typically increase proportionally with external salinity (Homayouni et al. 2024; Aghaleh et al. 2011). On the other hand, high salinity (60 g L^{-1} NaCl) reduced essential nutrients (particularly K^+, Ca^{2+}, P, and S) in both plant tissues and substrate. Excess Cl^- or Na^+ may affect the binding capacity of ions to soil particles, thereby promoting their loss through leaching. In addition, elevated NaCl concentrations in the soil solution may impair the uptake and accumulation of essential mineral nutrients, ultimately leading to disturbances in cellular homeostasis and functionality (Rahman et al. 2021). Excess Na^+ competes with Ca^{2+} at membrane binding sites, leading to disruptions in membrane stability, signaling processes, and enzyme function (Munns and Tester 2008). Nevertheless, it is widely recognized that Na^+ and Cl^- are largely sequestered within vacuoles in halophyte plants, thereby maintaining cytoplasmic ion concentrations within physiologically acceptable limits (Flowers and Colmer 2008). Besides toxic ions compartmentation in vacuoles, K^+ and organic solutes, like proline and sugars in the cytoplasm, are crucial to assure osmotic adjustment in cells of halophytes in saline environments (Munns et al. 2019). Even though high salt treatment reduced K^+ and Ca^{2+} contents in both shoots and roots, *S. lagascae* plants were able to maintain substantial levels of these macronutrients despite the high Na^+ accumulation detected in these organs. This response is typical of many halophytes, which can tolerate and accumulate large amounts of toxic ions, particularly in the shoots. In this regard, it has been reported that some halophytes are capable of using Na^+ instead of K^+ for turgor regulation in guard cells (Ozfidan-Konakci et al. 2016).

Increasing salinity from 30 to 60 g L^{-1} NaCl resulted in a general decline of essential macronutrients, especially K^+ and Ca^{2+}, leading to increased Na^+/K^+ and Na^+/Ca^{2+} ratios in shoots and roots, especially in L plants (Fig. 2). S plants maintained higher K^+ levels, whereas L plants showed a stronger decline under high salinity, suggesting reduced capacity to regulate Na^+/K^+ and Na^+/Ca^{2+} balance. This nutrient imbalance may affect osmotic regulation, enzyme activation, and membrane selectivity, as K^+ is critical for cellular homeostasis and Ca^{2+} for membrane stability and signaling.

Salinity also affected P and S homeostasis, with reduced phosphate and sulphate levels potentially linked to impaired uptake and metabolic adjustments under stress (Martínez and Läuchli 1994; Hongqiao et al. 2021). Although P is not typically considered the most limiting nutrient for plant growth, it has been shown to constrain growth in *Salicornia* species when present at low concentrations Brown et al. (2006). A reduction in sulphate uptake may impair S-dependent biosynthesis and disrupt cellular redox homeostasis, as evidenced by the decline in shoot glutathione (GSH) levels (Hongqiao et al. 2021). Thus, the salt-induced symptoms observed in plants under 60 g L^{-1} NaCl compared with 30 g L^{-1} NaCl may be associated with salinity-induced nutrient imbalances, particularly involving Ca^{2+}, K^+, P and S (including phosphate and sulphate), especially in shoots, due to their essential roles in plant metabolism (Marschner 1995).

4.3. Antioxidant defense system

It is well established that salt stress induces an oxidative stress at subcellular level, characterized by excessive production of reactive oxygen species (ROS) and increased lipid peroxidation (Hernández et al. 1993, 1995, 2001; Mittova et al. 2003). However, *S. lagascae* did not exhibit increased lipid peroxidation under high salinity, despite visible salt-induced injury in plants exposed to 60 g L^{-1} NaCl. Although reduced Ca^{2+} levels would compromise membrane integrity due to competition between Na^+ and Ca^{2+} at membrane binding sites (Munns and Tester 2008), membrane stability integrity appeared to be preserved. These results suggest that *S. lagascae* preserves membrane functionality through effective ion compartmentalization and stabilization mechanisms.

S. lagascae plants displayed an active antioxidant machinery, including the ASC-GSH cycle enzymes together with CAT, POX, and SOD activities. APX activity is a key component of salt tolerance due to its subcellular distribution and role in ROS detoxification (Jiménez et al., 1997; Hernández et al. 2000, 2001). In this regard, it is well reported that salinity negatively affect APX activity in different plant species (Hernández et al. 2001; Acosta-Motos et al. 2015; Cantabella et al. 2017). In this study, high salinity caused a 40% decline in APX activity in both S and L plants, potentially limiting H_2O_2 scavenging. Moreover, the decline in APX activity under 60 g L^{-1} NaCl correlated with reduced K^+ content in shoots, suggesting a potential link between K^+ depletion and impaired antioxidant capacity. Potassium plays a crucial role in regulating enzyme activation, osmotic balance, and ROS detoxification (Cakmak 2005; Wang et al. 2013). In contrast, K^+ deficiency in the halophyte *Cakile maritima*, has been reported to trigger oxidative stress with a concomitant increase in APX, MDHAR and SOD activities (Houmany et al. 2022). The discrepancy between these findings and our results may reflect differences in experimental conditions, particularly the higher NaCl concentrations used in this study, as well as species-specific physiological responses to salinity and nutrient imbalance. Nevertheless, despite lower APX activity, under 60 g L^{-1} NaCl plants maintained substantial enzymatic antioxidant capacity, and no oxidative membrane damage was detected. These results indicate that antioxidant defences remained sufficiently active to preserve cellular homeostasis. In addition, both S and L plants retained POX and SOD activities under hypersaline stress, indicating an effective regulation of H_2O_2 and $O_2.^-$, as reflected in the lack of membrane damage.

On the other hand, a significant increase in CAT activity was observed in L60 plants, suggesting enhanced H_2O_2 detoxification in peroxisomes, possibly linked to increased photorespiration under high salinity and thereby preventing its diffusion into the cytosol. Comparable increases in CAT activity have been previously reported in other halophytic species exposed to NaCl concentrations ranging from 300 to 600 mM (Ben Hsouna et al. 2000; Yildiz and Terzi, 2021; Mann et al. 2021).

Interestingly, under 30 g L^{-1} NaCl, S and L plants appeared to rely on different ascorbate recycling strategies. In this regard, L30 plants exhibited higher MDHAR activity, suggesting enhanced NADH-dependent ASC recycling, whereas S30 plants showed greater DHAR activity, which would indicate a higher energetic cost for ascorbate recycling. Moreover, the absence of changes of DHAR and GR activities in response to salinity (key enzymes involved in ascorbate and glutathione recycling) and on lipid peroxidation suggests that *S. lagascae* is able to maintain redox homeostasis under hypersaline stress conditions.

Isoenzyme analyses also revealed differences between plant types. S plants exhibited an additional low-mobility POX isoenzyme absent in L plants. Moreover, L60 plants showed reduced intensity of the Cu,Zn-SOD II isoenzyme, coinciding with the strongest decline in K^+ levels. Similar reductions in Cu,Zn-SOD isoenzymes under salinity have been reported in *S. europaea* (Aghaleh et al.,

2011), suggesting that K^+ depletion may influence specific antioxidant isoforms under salt stress. Thus, overall, *S. lagascae* maintained membrane integrity and metabolic homeostasis under high salinity through efficient ROS regulation and coordinated antioxidant responses. Although APX activity declined together with Ca^{2+} and K^+ levels, sustained SOD, POX, DHAR, GR, and CAT activities suggest a well-coordinated antioxidant defense system, contributing to the absence of oxidative damage and the salt tolerance of this species.

5. Metabolomic responses of Salicornia lagascae under salinity stress

At the metabolomic level, S30 plants showed a marked metabolic reprogramming, characterized by the enrichment of both primary and secondary metabolic pathways, in comparison to S60, L30 and L60 plants, whose profiles grouped together in clustering and hierarchical analyses. Concerning primary metabolism, butanoate metabolism, C5-branched dibasic acid metabolism, arginine and proline metabolism, galactose metabolism, and monoterpenoid biosynthesis were affected in S30 with respect to the rest of the treatments. These changes indicate coordinated adjustments in carbon flux, organic acid turnover, amino acid interconversion, sugar metabolism, and terpene biosynthesis, collectively reflecting a reorganization of carbon and nitrogen metabolism. Such metabolic shifts are widely associated with plant responses to environmental and growth-related changes (Fiehn 2002; Atrous et al. 2026; Barba-Espin et al. 2025; Jurado-Mañogil et al. 2023).

In contrast, under *in vitro* conditions, we recently reported that liquid medium propagation induced pronounced metabolomic changes associated with enhanced micronutrient accumulation, improved rhizogenesis, and increased plant growth (Atrous et al., 2026). Thus, the absence of such metabolomic differences in this study are likely a result of the higher adaptation of plants to liquid micropropagation, reducing the need for large-scale metabolic adjustments after transplantation.

A tight relationship between amino acid metabolism and stress responses has been reported (Batista-Silva et al. 2018; Hildebrandt et al. 2015). Under limited carbohydrate availability, amino acids serve as alternative substrates for mitochondrial respiration, with proline catabolism supporting ATP production and generating 2-oxoglutarate as a tricarboxylic acid (TCA) intermediate, contributing to stress tolerance and redox buffering (Batista-Silva et al., 2018; Hildebrandt et al. 2015). A prominent feature observed in S30 shoots was the enrichment of pathways related to amino acid metabolism, particularly branched-chain amino acids (BCAAs). In plants, this mitochondrial pathway is involved in the degradation of BCAAs, particularly Leu, but also Ile and Val. Degradation of these amino acids generates intermediates that feed into the TCA cycle, thereby supporting mitochondrial respiration and energy production under stress conditions (Binder et al. 2010). Although BCAAs participate in primary metabolism and can contribute to the synthesis of specialized metabolites and signalling molecules (Hildebrandt et al. 2015), under salt stress BCAA metabolism primarily supports metabolic flexibility by linking amino-acid catabolism with central energy metabolism (Huang and Jander 2015). Untargeted metabolomics studies in salt-stressed plants, including *Portulaca oleracea*, identify this pathway as significantly enriched in response to salinity (Belo Silva et al. 2022). In addition, BCAAs catabolism generates CoA-linked products that can feed directly into the TCA cycle, providing carbon skeletons for energy production and intermediary metabolism (Zhang et al. 2017). Similar salinity-induced increases in TCA cycle components were reported in the halophyte *Sesuvium portulacastrum* (Kulkarni et al. 2022). The enrichment of butanoate metabolism in S30 plants further supports this interpretation. In plants this pathway integrates peroxisomal fatty acid β-oxidation, the mitochondrial γ-aminobutyric acid (GABA) shunt and the TCA cycle. Activation of the GABA shunt provides an alternative route for carbon entry into the TCA cycle contributing to the maintenance of C/N balance. The coordinated enrichment of amino acid and butanoate metabolism therefore indicates a tight coupling between nitrogen metabolism and energy production in S30 plants (Flaherty and Shelp 2026; Shelp et al. 2011).

Moreover, the enrichment of galactose metabolism in S30 shoots suggests increased synthesis of compatible solutes such as raffinose and stachyose, which contribute to osmotic adjustment and membrane stabilization (Keunen et al. 2013; ElSayed et al. 2014). In parallel, alteration of monoterpenoid and steroid biosynthesis pathways in S30 plants may be contributing to membrane stabilization and stress signalling (Du et al., 2022). An increase in stigmasterol, isofucosterol, and avenasterol contents occurred in S30 shoots. Similar sterol accumulation has been reported in the salt-tolerant species *Brassica napus*, *B. oleracea* and *Cakile maritima* in response to salinity (Chalbi et al. 2015). Such changes are consistent with membrane stabilization mechanisms that contribute to salinity tolerance in halophytic species. In contrast, in the glycophytic *Glycine max*, salinity reduced sterol contents in roots (Surjus and Durand 1996), while exogenous application of stigmasterol or sitosterol has been reported to alleviate salt-induced damage in flax and pepper plants (Hashem et al. 2011; Abu-Miriefah 2015).

Enhanced flavonoid and polyamine metabolism in S30 shoots indicates a metabolic shift toward specialized secondary metabolism associated with oxidative an osmotic stress protection (Tohge et al. 2017). In halophytes, flavonol derivatives often represent an important component of the antioxidant defence system. For instance, in *Salicornia europaea*, quercetin glycosides increased markedly under high salt stress, while free kaempferol declined alongside a concomitant rise in its glycosylated derivates, suggesting a restructuring of the flavonol profile toward compounds with greater ROS-scavenging capacity under severe salinity (Duan et al. 2023). A similar pattern occurs in *Atriplex canescens*, where total flavonoid content significantly increased in seedlings exposed to 100 and 300 mM NaCl, highlighting the contribution of flavonoid metabolism to salt adaptation (Feng et al. 2023). Supporting this biochemical evidence, ectopic overexpression of chalcone isomerase, a key enzyme in the flavonoid biosynthesis, from *A. canescens* in *Arabidopsis thaliana* enhanced tolerance to salt and osmotic stress, directly linking activation of the flavonoid pathway to improved stress resilience (Feng et al. 2023). Moreover, salt-induced polyamine accumulation contributes to osmotic and ionic stress tolerance by stabilizing membranes and scavenging ROS (Ikbal et al. 2014; Szabados and Savouré 2010).

Only a few metabolites were significantly down-regulated in S30 plants. The downregulation of tridec-7-enoic acid (C13:1) may reflect membrane lipid remodelling in response to moderate salinity, while the decrease in N-methyl-4-aminobutyric acid (a GABA derivate) alongside with the accumulation of succinic semialdehyde and succinate is consistent with enhanced GABA shunt activity, supporting carbon flux into the TCA cycle for energy production (Shelp et al. 2011, 2021). In the comparison between S30 and S60 plants, pyridoxine (vitamin B_6) accumulated under high salinity, reflecting an additional stress response. Vitamin B_6 is known to accumulate under severe stress conditions where it functions as an antioxidant and enzymatic cofactor (Herrero et al. 2011), although information about the role of pyridoxine in halophytes is very scarce.

Taken together, the metabolomic profile of S30 plants suggests a coordinated metabolic strategy integrating carbon reallocation, amino-acid turnover, osmoprotectant synthesis, membrane stabilization and antioxidant defence, which is closely associated with higher shoot Na^+ levels and increased root K^+ and P contents relative to the other treatments. This may reflect an adaptive metabolic response that enhanced ion homeostasis, metabolic flexibility, and stress tolerance in *S. lagascae*.

6. Conclusions

In summary, *in vitro* selection proved effective for identifying highly salt-tolerant *S. lagascae* clones, which maintained physiological stability, efficient photosynthesis, and antioxidant protection under high salinity conditions. Although high NaCl levels caused ionic imbalance, salinity-related symptoms, and metabolic adjustments, the plants preserved membrane integrity and sustained antioxidant capacity, thereby avoiding long-term oxidative damage.

Overall, *S. lagascae* exhibits a high degree of salt tolerance through the coordinated regulation of ion homeostasis, osmotic adjustment, photoprotective energy dissipation, antioxidant defenses, and metabolic reprogramming. These integrated mechanisms maintain cellular and redox homeostasis, preserve photosynthetic performance, and support adaptation to hypersaline environments even at NaCl concentrations as high as 60 g L^{-1}.

The S30 treatment generated the strongest metabolomic response, likely due to those plants grown under moderate salinity (30 g L^{-1} NaCl) experienced conditions close to the optimal salinity range reported for Salicornia species, whereas severe salinity reduced nutrient availability, especially K^+ and Ca^{2+}, and imposed stronger osmotic and ionic stress, which may have constrained metabolic flexibility. Furthermore, liquid micropropagation may reduce the need for ulterior major metabolic adjustments under *ex vitro* conditions.

Taken together, these results highlight the remarkable physiological and metabolic plasticity of *S. lagascae*, which maintains strong overall performance even at salinity levels as high as 60 g L^{-1} NaCl. Its ability to accumulate high concentrations of toxic ions in aerial tissues reinforce its resilience to severe salinity conditions. Importantly, these traits underscore the broader ecological and agronomic relevance of halophytes, supporting its potential for saline agriculture and restoration of salt-degraded environmen. Moreover, this work emphasizes the usefulness of *in vitro* culture as a strategy for selecting elite genotypes for hypersaline environments.

Declarations

Acknowledgements

This work was funded by the Partnership on Research and Innovation in the Mediterranean Area (PRIMA) programme, supported by the European Union, through the HaloFarMs project (PRIMA/0002/2019). Additional funding was provided by the Spanish State Research Agency (MCIN/AEI/10.13039/501100011033) through the R&D&I Projects International Joint Programming initiative (PCI2020-111977) and by MICIU/AEI/10.13039/501100011033 and by the European Union through the Biodiversa+ project SaltyBEATS (PCI2025-163138).

Author Contribution

GA: data curation, formal analysis, investigation, methodology; PDV: data curation, formal analysis, investigation, methodology, writing—review & editing, supervision; AP: conceptualization, investigation, methodology; AHC: investigation, methodology; GBE: data curation, formal analysis, investigation, methodology, writing—review & editing, supervision; JAH: data curation, formal analysis, investigation, methodology, writing—original draft, writing—review & editing, funding acquisition, project administration, resources, supervision.

Funding Open access funding provided by the CRUE-CSIC Alliance.

Conflict of interest The authors declare no competing interests

Data Availability Statement The datasets generated during and/or analysed during the current study are available from the corresponding author on reasonable request.

Declaration of generative AI use

During the preparation of this manuscript, the authors used ChatGPT to refine the English language and assist in the design of the graphical abstract. The authors carefully reviewed and edited all AI-generated content as necessary and take full responsibility for the content of the published article.

Ghofrane Atrous, https://orcid.org/0009-0002-3822-5961

Pedro Diaz-Vivancos, https://orcid.org/0000-0001-6041-2128

Ana Hernández-Cánovas, https://orcid.org/0009-0001-4860-9291

Gregorio Barba-Espín, https://orcid.org/0000-0001-9229-9668

José A. Hernández, https://orcid.org/0000-0001-7211-5147

References

1. Abu-Miriefah SS (2015) Effect of sitosterol on growth, metabolism and protein pattern of pepper (*Capsicum annuun* L.) plants growth under salt stress conditions. Int J Agric Crop Sci 8:94–106
2. Acosta-Motos JR, Ortuño MF, Álvarez S, López-Climent MF, Gómez-Cadenas A, Sánchez-Blanco MJ (2016) Changes in growth, physiological parameters and the hormonal status of *Myrtus communis* L. plants irrigated with water with different chemical compositions. J Plant Physiol 191:12–21. https://doi.org/10.1016/j.jplph.2015.11.010
3. Acosta-Motos JR, Noguera-Vera L, Barba-Espín G, Piqueras A, Hernández JA (2019) Antioxidant metabolism and chlorophyll fluorescence during the acclimatisation to ex vitro conditions of micropropagated *Stevia rebaudiana* Bertoni plants. Antioxidants 8:615. https://doi.org/10.3390/antiox8120615
4. Adelberg J, Kroggel M, Toler J (2000) Physical environment in vitro affects laboratory and nursery growth of micropropagated hostas. HortTechnology 10:754–757. https://doi.org/10.21273/HORTTECH.10.4.754
5. Aghaleh M, Niknam V, Ebrahimzadeh H, Razavi K (2011) Effect of salt stress on physiological and antioxidative responses in two species of Salicornia (S. persica and S. europaea). Acta Physiol Plant 33:1261–1270. https://doi.org/10.1007/s11738-011-0677-0
6. Akhtar MT, Noor M, Lin X, Lu Z, Jin B (2026) Flavonoids in plant salt stress responses: biosynthesis, regulation, functions, and signaling networks. Plants 15:171. https://doi.org/10.3390/plants15010171
7. Atrous G, Piqueras A, Díaz-Vivancos P, Hernández-Cánovas A, Hamed KB, Hernández JA, Barba-Espín G (2025) In vitro-selected clones of the halophyte Arthrocaulon macrostachyum display enhanced salinity stress tolerance. Plants 14:1164.

https://doi.org/10.3390/plants14081164

8. Atrous G, Barba-Espín G, Piqueras A, Hernández JA, Díaz-Vivancos P (2026) Cultivation of Salicornia lagascae in high-NaCl liquid medium induces a metabolic reprogramming and enhances micropropagation performance. J Plant Growth Regul. https://doi.org/10.1007/s00344-026-12176-1
9. Barba-Espín G, Jurado-Mañogil C, Plskova Z, Kerchev PI, Hernández JA, Díaz-Vivancos P (2025) Halophyte-based crop-managements induce biochemical, metabolomic and proteomic changes in tomato plants under saline conditions. Physiol Plant 177:e70060. https://doi.org/10.1111/ppl.70060
10. Batista-Silva W, Heinemann B, Rugen N, Nunes-Nesi A, Araújo WL, Braun HP, Hildebrandt TM (2018) The role of amino acid metabolism during abiotic stress responses. Plant Cell Environ 42:1630–1644. https://doi.org/10.1111/pce.13518
11. Bazihizina N, Papenbrock J, Aronsson H, Ben Hamed K, Elmaz O, Dafku Z, Custódio L, Rodrigues MJ, Atzori G, Negacz K (2024) The sustainable use of halophytes in salt-affected land: state-of-the-art and next steps in a saltier world. Plants 13:2322. https://doi.org/10.3390/plants13162322
12. Ben Hsouna A, Ghneim-Herrera T, Ben Romdhane W, Dabbous A, Ben Saad R, Brini F, Abdelly C, Ben Hamed K (2020) Early effects of salt stress on the physiological and oxidative status of the halophyte Lobularia maritima. Funct Plant Biol 47:912–924. https://doi.org/10.1071/FP19303
13. Bhaskara GB, Yang TH, Verslues PE (2015) Dynamic proline metabolism: importance and regulation in water-limited environments. Front Plant Sci 6:484. https://doi.org/10.3389/fpls.2015.00484
14. Belo Silva VN, Carvalho da Silva TL, Malheiros Ferreira TM, Rodrigues Neto JC, Pereira Leão A, de Aquino Ribeiro JA, Verardi Abdelnur P, Fonseca Valadares L, Ferreira de Sousa CA, Teixeira Souza Júnior M (2022) Multi-omics analysis of young Portulaca oleracea plants' responses to high NaCl doses reveals insights into pathways and genes responsive to salinity stress in this halophyte species. Phenomics 3:1–21
15. Binder S (2010) Branched-chain amino acid metabolism in Arabidopsis thaliana. Arabidopsis Book 8:e0137
16. Brown CE, Pezeshki SR, DeLaune RD (2006) The effects of salinity and soil drying on nutrient uptake and growth of Spartina alterniflora in a simulated tidal system. Environm Exp Bot 58:140–148. https://doi.org/10.1016/j.envexpbot.2005.07.006
17. Cantabella D, Piqueras A, Acosta-Motos JR, Bernal-Vicente A, Hernández JA, Díaz-Vicancos P (2017) Salt-tolerance mechanisms induced in Stevia rebaudiana Bertoni: effects on mineral nutrition, antioxidative metabolism and steviol glycoside content. Plant Physiol Biochem 115:484–496. https://doi.org/10.1016/j.plaphy.2017.04.023
18. Chalbi N, Martínez-Ballesta MC, Youssef NB, Carvajal M (2015) Intrinsic stability of Brassicaceae plasma membrane in relation to changes in protein and lipids in response to salinity. J Plant Physiol 175:148–156. https://doi.org/10.1016/j.jplph.2014.12.003
19. Custódio L, Charles G, Magné C, Barba-Espín G, Piqueras A, Hernández JA, Ben Hamed K, Castañeda-Loaiza V, Fernandes E, Rodrigues MJ (2023) Application of *in vitro* plant tissue culture techniques to halophyte species: a review. Plants 12:126. https://doi.org/10.3390/plants12010126
20. de Jesus Raposo MF, de Morais RMSC (2021) Micropropagation of the halophyte *Sarcocornia fruticosa* (L.) A.J. Scott. J Basic Appl Sci 10:53–59
21. Du Y, Fu X, Chu Y, Wu P, Liu Y, Ma L, Tian H, Zhu B (2022) Biosynthesis and the roles of plant sterols in development and stress responses. Int J Mol Sci 23:2332. https://doi.org/10.3390/ijms23042332
22. Duan H, Tiika RJ, Tian F, Lu Y, Zhang Q, Hu Y, Cui G, Yang H (2023) Metabolomics analysis unveils important changes involved in the salt tolerance of Salicornia europaea. Front Plant Sci 13:1097076. https://doi.org/10.3389/fpls.2022.1097076
23. Duarte B, Santos D, Marques JC, Caçador I (2013) Ecophysiological adaptations of two halophytes to salt stress: photosynthesis, PSII photochemistry and antioxidant feedback—implications for resilience in climate change. Plant Physiol Biochem 67:178–188
24. FAO (2021) Global map of salt-affected soils. Available at: https://www.fao.org/3/cb7247en/cb7247en.pdf
25. FAO (2024) Global status of salt-affected soils - Main report. Rome. https://doi.org/10.4060/cd3044en https://doi.org/10.4060/cd3044en
26. Feng S, Yao YT, Wang BB, Li YM, Guo H, Bao AK (2023) Flavonoids are involved in salt tolerance through ROS scavenging in the halophyte *Atriplex canescens*. Plant Cell Rep 43:1–18. https://doi.org/10.1007/s00299-023-03087-6
27. Fiehn O (2002) Metabolomics – the link between genotypes and phenotypes. Plant Mol Biol 48:155–171. https://doi.org/10.1023/A:1013713905833

28. Flaherty EJ, Shelp BJ (2026) Interaction of 4-aminobutyrate (GABA) with the tricarboxylic acid cycle in plants under salinity stress. Plants 15:123. https://doi.org/10.3390/plants15010123
29. Flowers TJ, Colmer TD (2008) Salinity tolerance in halophytes. New Phytol 179:945–963. https://doi.org/10.1111/j.1469-8137.2008.02531.x
30. Gulzar B, Mujib A, Qadir Malik M, Mamgain J, Syeed R, Zafar N (2020) Plant tissue culture: agriculture and industrial applications. In: Kiran U, Abdin MZ, Kamaluddin (eds) Transgenic technology-based value addition in plant biotechnology. Academic, New York, pp 25–49. https://doi.org/10.1016/B978-0-12-818632-9.00002-2
31. Hashem HA, Bassuony FM, Hassanein RA, Baraka DM, Khalil RR (2011) Stigmasterol seed treatment alleviates the drastic effect of NaCl and improves quality and yield in flax plants. Aust J Crop Sci 5:1858–1867
32. Hernández JA, Corpas FJ, Gómez M, Del Río LA, Sevilla F (1993) Salt-induced oxidative stress mediated by activated oxygen species in pea leaf mitochondria. Plant Physiol 89:103–110
33. Hernández JA, Olmos E, Corpas FJ, Sevilla F, Del Río LA (1995) Salt-induced oxidative stress in chloroplasts of pea plants. Plant Sci 105:151–167
34. Hernández JA, Campillo A, Jiménez A, Alarcón JJ, Sevilla F (1999) Response of antioxidant systems and leaf water relations to NaCl stress in pea plants. New Phytol 141:241–251
35. Hernández JA, Jiménez A, Mullineaux PM, Sevilla F (2000) Tolerance of pea (*Pisum sativum* L.) to long-term salt stress is associated with induction of antioxidant defenses. Plant Cell Environ 23:853–862
36. Hernández JA, Ferrer MA, Jiménez A, Ros-Barceló A, Sevilla F (2001) Antioxidant systems and $O_2{\bullet}^-/H_2O_2$ production in the apoplast of *Pisum sativum* L. leaves: its relation with NaCl-induced necrotic lesions in minor veins. Plant Physiol 127:817–831
37. Herrero S, González E, Gillikin JW, Vélëz H, Daub ME (2011) Identification and characterization of a pyridoxal reductase involved in the vitamin B6 salvage pathway in Arabidopsis. Plant Mol Biol 76:157–169
38. Hildebrandt TM, Nunes-Nesi A, Araújo WL, Braun HP (2015) Amino acid catabolism in plants. Mol Plant 8:1563–1579. https://doi.org/10.1016/j.molp.2015.09.005
39. Homayouni H, Razi H, Izadi M, Alemzadeh A, Kazemeini SA, Niazi A, Vicente O (2024) Temporal changes in biochemical responses to salt stress in three Salicornia species. Plants 13:979
40. Hongqiao L, Suyama A, Mitani-Ueno N, Hell R, Maruyama-Nakashita A (2021) A low level of NaCl stimulates plant growth by improving carbon and sulphur assimilation in *Arabidopsis thaliana*. Plants 10:2138. https://doi.org/10.3390/plants10102138
41. Houmani H, Debez A, Freitas-Silva LD, Abdelly C, Palma JM, Corpas FJ (2022) Potassium (K^+) starvation-induced oxidative stress triggers a general boost of antioxidant and NADPH-generating systems in the halophyte *Cakile maritima*. Antioxidants 11:401. https://doi.org/10.3390/antiox11020401
42. Huang T, Jander G (2017) Abscisic acid-regulated protein degradation causes osmotic stress-induced accumulation of branched-chain amino acids in Arabidopsis thaliana. Planta 246:737–747. https://doi.org/10.1007/s00425-017-2727-3
43. Ikbal F, Hernández JA, Barba-Espín G, Koussa T, Aziz A, Faize M, Díaz-Vivancos P (2014) Enhanced salt-induced antioxidative responses involve a contribution of polyamine biosynthesis in grapevine plants. J Plant Physiol 171:779–788
44. Jimenez A, Hernandez JA, del Río LA, Sevilla F (1997) Evidence for the presence of the ascorbate–glutathione cycle in mitochondria and peroxisomes of pea (*Pisum sativum* L.) leaves. Plant Physiol 114:275–284
45. Jordine A, Retzlaff J, Gens L, Ehrt B, Fürtauer L, van Dongen JT (2024) Introducing the halophyte *Salicornia europaea* to investigate combined impact of salt and tidal submergence conditions. Funct Plant Biol 51:FP23228
46. Jurado C, Díaz-Vivancos P, Gregorio BE et al (2024) Effect of halophyte-based management in physiological and biochemical responses of tomato plants under moderately saline greenhouse conditions. Plant Physiol Biochem 206:108228. https://doi.org/10.1016/j.plaphy.2023.108228
47. Jurado-Mañogil C, Barba-Espín G, Hernández JA, Díaz-Vivancos P (2023) Comparative metabolomic analysis between tomato and halophyte plants under intercropping conditions. Physiol Plant 175:e13971. https://doi.org/10.1111/ppl.13971
48. Jurado-Mañogil C, Díaz-Vivancos P, Hernández JA et al (2024) Efficient in vitro platform for multiplication, acclimatization, and delivery of high-NaCl-tolerant clones of the halophyte *Arthrocaulon macrostachyum*. J Plant Growth Regul 43:1631–1641. https://doi.org/10.1007/s00344-023-11210-w
49. Kulkarni J, Sharma S, Sahoo SA, Mishra S, Nikam TD, Borde M, Penna S, Srivastava AK (2022) Resilience in primary metabolism contributes to salt stress adaptation in *Sesuvium portulacastrum* L. J Plant Growth Regul 98:385–398

50. Liu CZ, Murch SJ, El-Demerdash M, Saxena PK (2004) *Artemisia judaica* L.: micropropagation and antioxidant activity. J Biotechnol 110:63–71. https://doi.org/10.1016/j.jbiotec.2004.01.011
51. Mann A, Kumar N, Kumar A, Lata C, Kumar A, Meena BL, Mishra D, Grover M, Gaba S, Parameswaran C et al (2021) De novo transcriptomic profiling of differentially expressed genes in grass halophyte Urochondra setulosa under high salinity. Sci Rep 11:1–14
52. Marschner H (1995) Mineral nutrition of higher plants, 2nd edn. Academic, London, pp 379–396
53. Martinez V, Läuchli A (1994) Salt-induced inhibition of phosphate uptake in plants of cotton (*Gossypium hirsutum* L). New Phytol 125:609–614. https://doi.org/10.1111/j.1469-8137.1994.tb03814.x
54. Mbiyu M, Muthoni J, Kabira J et al (2012) Comparing liquid and solid media on the growth of plantlets from three Kenyan potato cultivars. J Exp Agric Int 2:81–89
55. Mittova V, Tal M, Volokita M, Guy M (2003) Up-regulation of the leaf mitochondrial and peroxisomal antioxidative systems in response to salt-induced oxidative stress in the wild salt-tolerant tomato species *Lycopersicon pennellii*. Plant Cell Environ 26:845–856. https://doi.org/10.1046/j.1365-3040.2003.01016.x
56. Munns R, Tester M (2008) Mechanisms of salinity tolerance. Annu Rev Plant Biol 59:651–681. https://doi.org/10.1146/annurev.arplant.59.032607.092911
57. Munns R, Passioura JB, Colmer TD, Byrt CS (2019) Osmotic adjustment and energy limitations to plant growth in saline soil. New Phytol 225:1091–1096. https://doi.org/10.1111/nph.15862
58. Noctor G (2006) Metabolic signalling in defence and stress: the central roles of soluble redox couples. Plant Cell Environ 29:409–425
59. Pretty J, Benton TG, Bharucha ZP et al (2018) Global assessment of agricultural system redesign. Nat Sustain 1:441–446
60. Ozfidan-Konakci C, Uzilday B, Ozgur R et al (2016) Halophytes as a source of salt tolerance genes and mechanisms: a case study for the Salt Lake area, Turkey. Funct Plant Biol 43:575–589. https://doi.org/10.1071/FP15288
61. Ozel C, Khawar KM, Arslan O (2008) A comparison of isubgol, agar and gelrite on in vitro shoot regeneration and rooting of *Nicotiana tabacum* L. variety Samsun. Sci Hortic 117:174–181. https://doi.org/10.1016/j.scienta.2008.03.022
62. Rahman MM, Mostofa MG, Keya SS, Siddiqui MN, Ansary MMU, Das AK, Rahman MA, Tran LSP (2021) Adaptive mechanisms of halophytes and their potential in improving salinity tolerance in plants. Int J Mol Sci 22:10733
63. Ros Barceló A (1998) The generation of H_2O_2 in the xylem of Zinnia elegans is mediated by an NADPH-oxidase-like enzyme. Planta 207:207–216
64. Ruan CJ, Teixeira da Silva JA, Mopper S, Qin P, Lutts S (2010) Halophyte improvement for a salinized world. Crit Rev Plant Sci 29:329–359
65. Shabala S, Mackay A (2011) Ion transport in halophytes. Adv Bot Res 57:151–187
66. Shelp BJ, Mullen RT, Waller JC (2012) Compartmentation of GABA metabolism raises intriguing questions. Trends Plant Sci 17:57–59. https://doi.org/10.1016/j.tplants.2011.12.006
67. Shi H, Xiong L, Stevenson B, Lu T, Zhu JK (2002) The Arabidopsis salt overly sensitive 4m mutants uncover a critical role for vitamin B6 in plant salt tolerance. Plant Cell 14:575–588
68. Shuyskaya E, Rakhmankulova Z, Prokofieva M, Kazantseva V, Lunkova N (2023) Impact of salinity, elevated temperature, and their interaction on the photosynthetic efficiency of halophyte crop *Chenopodium quinoa* Willd. Agriculture 13:1198
69. Surjus A, Durand M (1996) Lipid changes in soybean root membranes in response to salt treatments. J Exp Bot 47:17–23. https://doi.org/10.1093/jxb/47.1.17
70. Szabados L, Savouré A (2010) Proline: a multifunctional amino acid. Trends Plant Sci 15:89–97. https://doi.org/10.1016/j.tplants.2009.11.009
71. Savchenko T, Walley JW, Chehab EW, Xiao Y, Kaspi R, Pye MF, Mohamed ME, Lazarus CM, Bostock RM, Dehesh K (2010) Arachidonic acid: an evolutionarily conserved signaling molecule modulates plant stress signaling networks. Plant Cell 22:3193–3205
72. Tohge T, de Souza LP, Fernie AR (2017) Current understanding of the pathways of flavonoid biosynthesis in plants. J Exp Bot 68:4013–4028. https://doi.org/10.1093/jxb/erx177

73. Vyas KD, Ranawat B, Singh A (2021) Development of high-frequency cost-effective micropropagation protocol for Juncus rigidus using liquid culture medium and extraction of cellulose from *in vitro* shoots—an important rush. Biocatal Agric Biotechnol 35:102099
74. Wungrampha S, Joshi R, Singla-Pareek SL, Pareek A (2018) Photosynthesis and salinity: are these mutually exclusive? Photosynthetica 56:366–381. https://doi.org/10.1007/s11099-017-0763-7
75. Yao L, Wang J, Yang K, Li B, Meng Y, Ma X, Lai Y, Si E, Ren P, Shang X et al (2021) In vitro regeneration system of *Halogeton glomeratus*: an important halophyte. Vitro Cell Dev Biol Plant 57:332–340
76. Yıldız M, Terzi H (2021) Comparative analysis of salt-induced changes in the root physiology and proteome of the xero-halophyte *Salsola crassa*. Braz J Bot 44:33–42. https://doi.org/10.1007/s40415-020-00695-4
77. Zhang S, Zeng X, Ren M, Mao X, Qiao S (2017) Novel metabolic and physiological functions of branched-chain amino acids: a review. J Anim Sci Biotechnol 8:10. https://doi.org/10.1186/s40104-016-0139-z
78. Zheleznichenko TV, Muraseva DS, Erst AS, Kuznetsov AA, Kulikovskiy MS, Kostikova VA (2023) The influence of solid and liquid systems in vitro on the growth and biosynthetic characteristics of microshoot culture of *Spiraea betulifolia* ssp. aemiliana. Int J Mol Sci 24:2362. https://doi.org/10.3390/ijms24032362

Figures

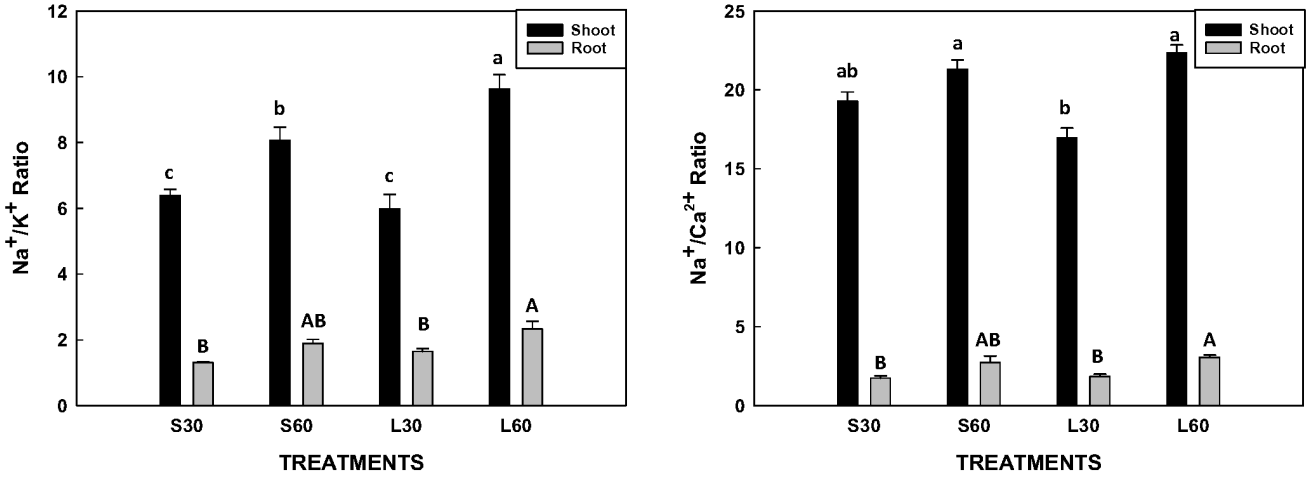


Figure 1

Effect of 30 and 60 g L^{-1} NaCl treatments on the Na^+/K^+ ratio (A) and the Na^+/Ca^{2+} ratio (B) in shoots and roots of *S. lagascae* plants derived from solid (S) or liquid (L) culture media. Data represent the mean ± SE of six plants. Different letters within the same column type indicate significant differences according to Tukey's multiple range test ($p \leq 0.05$). S30 and S60: acclimated plants from solid media treated with 30 g L-1 NaCl and 60 30 g L-1 NaCl, respectively; L30 and L60: acclimated plants from liquid media treated with 30 g L-1 NaCl and 60 g L-1 NaCl, respectively.

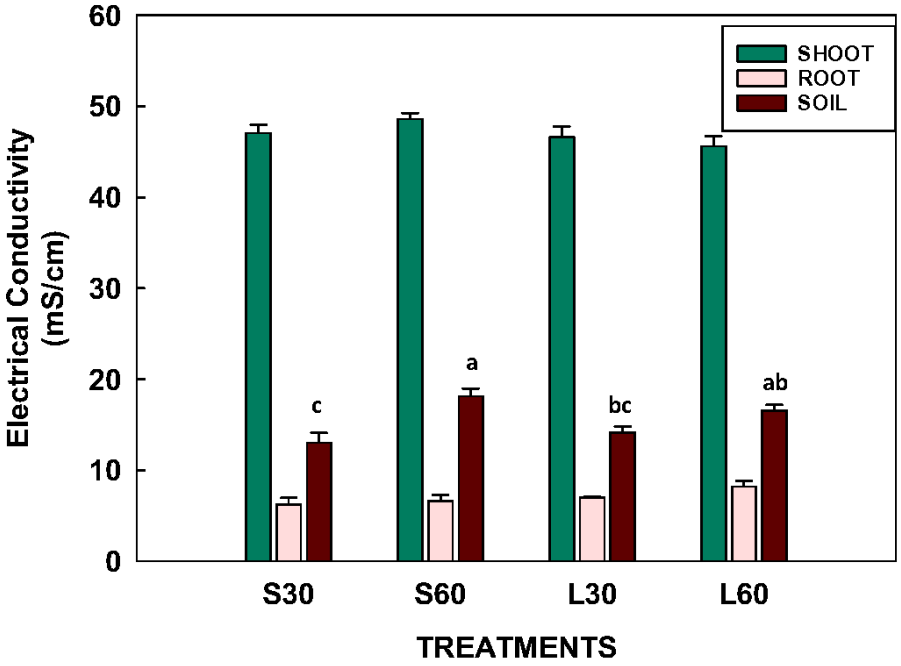


Figure 2

Effect of NaCl stress on the electrical conductivity of shoots and roots of *S. lagascae* plants as well as in the soil after 6 weeks (42 days) of treatments. Data represent the mean ± SE from six plants. Different letters in the same type of columns indicate significant differences according to Tukey's multiple range test ($p \leq 0.05$). S30 and S60: acclimated plants from solid media treated with 30 g L-1 NaCl and 60 30 g L-1 NaCl, respectively; L30 and L60: acclimated plants from liquid media treated with 30 g L-1 NaCl and 60 g L-1 NaCl, respectively.

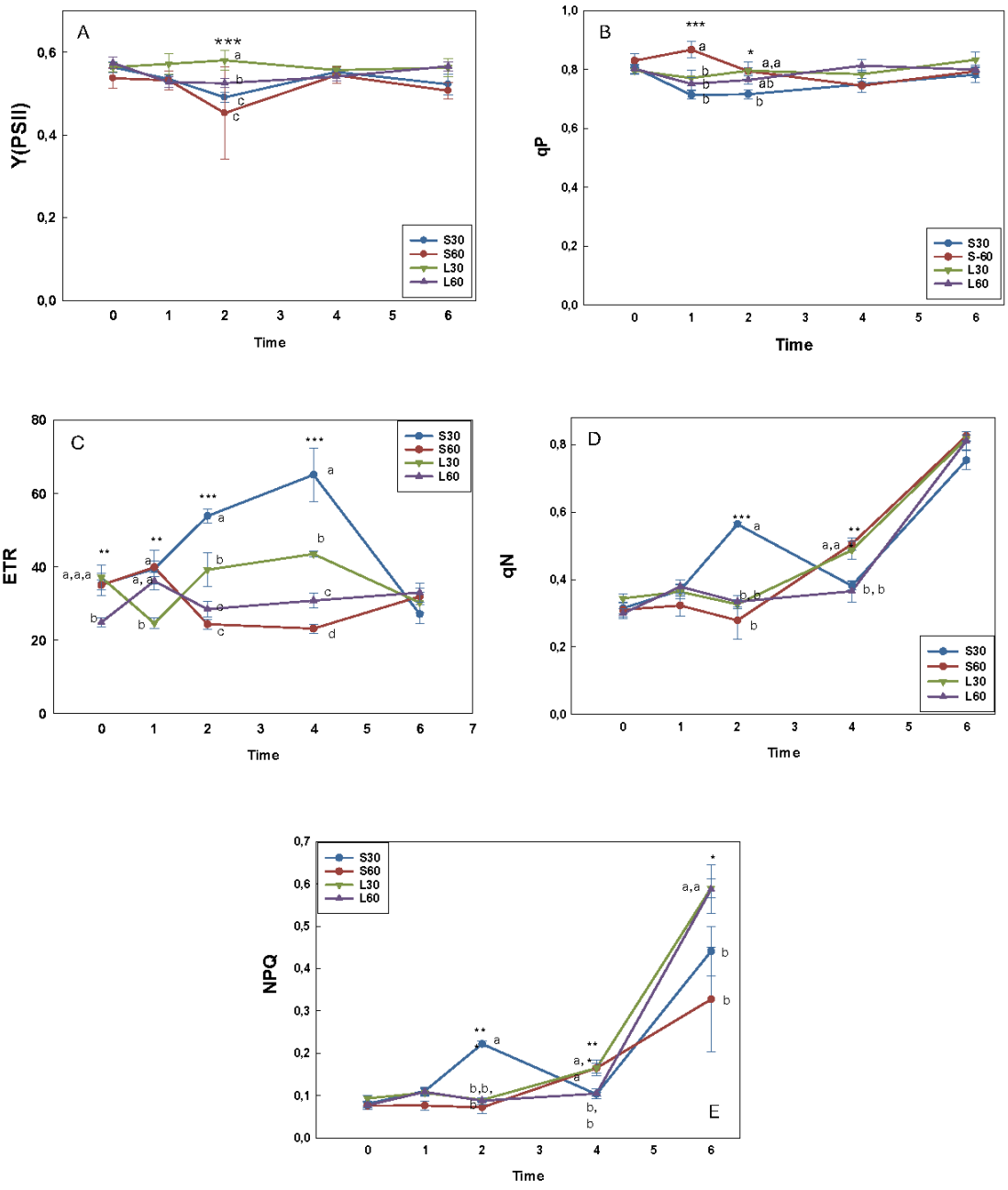


Figure 3

Effect of salinity on the effective PSII quantum yield [Y(II)], the coefficient of photochemical quenching (qP), the electron transport rate (ETR), the coefficient of non-photochemical quenching (qNP) and the non-photochemical quenching parameter (NPQ), in acclimated *Salicornia lagascae* plants rooted in solid (S) or liquid (L) media. Acclimated plants were treated with 30 g/L NaCl during 7 days. Then, half of the plants from each S or L media were treated with 30 g/L NaCl or 60 g/L NaCl respectively during 6 weeks. Data represent mean values ± standard error. S30 and S60: micropropagated on solid medium in the presence of 30 g/L and 60 g/L NaCl, respectively; L30 and L60: Plants micropropagated in liquid medium in the presence of 30 g/L and 60 g/L NaCl, respectively. 0, day 0; 1, day 7, 2 day 14, 4, day 28 and 5, day 42 of the experiment.

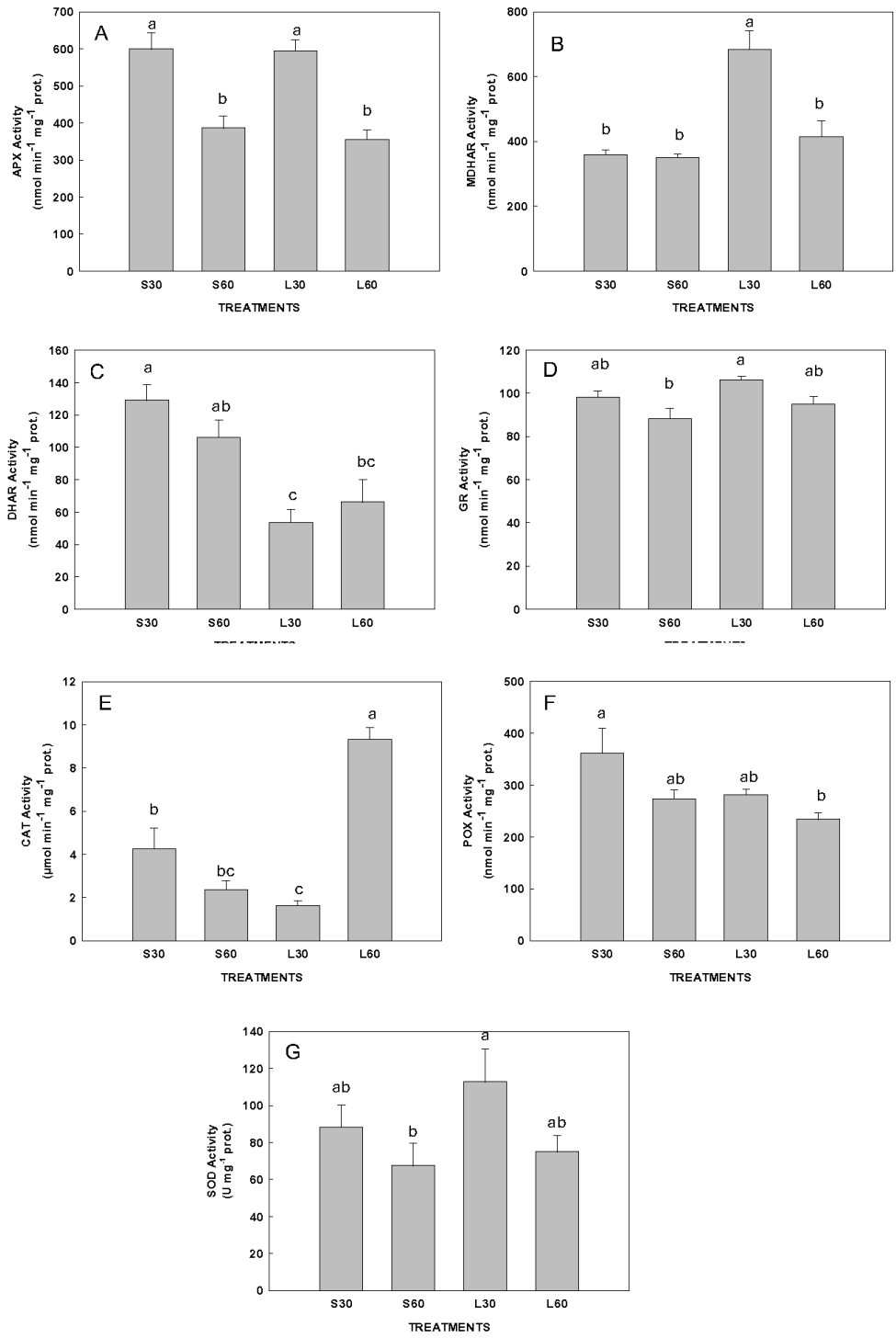


Figure 4

Effect of NaCl stress on the activity of the ASC-GSH cycle enzymes (A-D), CAT (E), POX (F) and SOD (F) from *S. lagascae* shoots, derived from solid (S) or liquid (L) culture media, after 6 weeks of treatments. Data represent the mean ± SE from five different biological samples. Different letters indicate significant differences according to Tukey's multiple range test ($p \leq 0.05$). S30 and S60: micropropagated on solid medium in the presence of 30 g/L and 60 g/L NaCl, respectively; L30 and L60: Plants micropropagated in liquid medium in the presence of 30 g/L and 60 g/L NaCl, respectively.

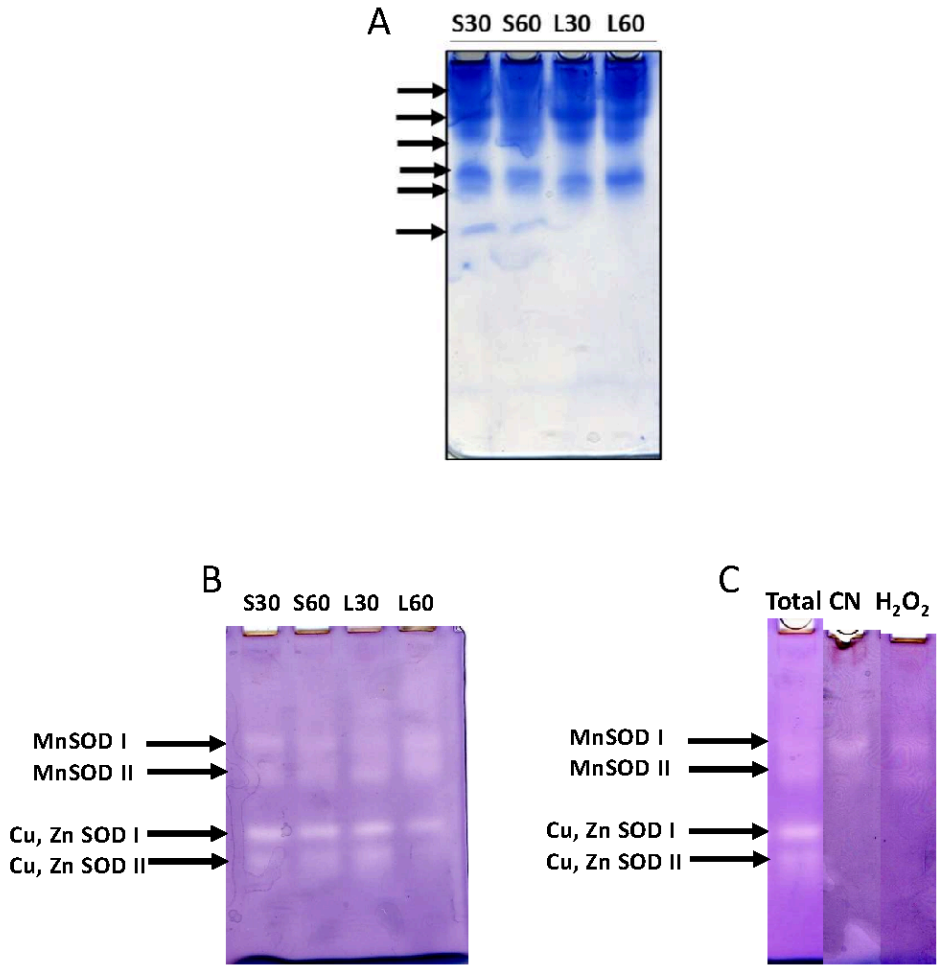


Figure 5

Effect of 30 and 60 g L^{-1} NaCl treatments on the pattern of native peroxidase isozymes (A) and on the isozyme pattern of superoxide dismutase (B) detected by native PAGE in *S. lagascae* shoots derived from solid (S) or liquid (L) culture media. C: Gels were stained in the presence and in the absence of KCN or H_2O_2 for SOD isoenzyme identification. A total of 70 micrograms of proteins were loaded in each lane. S30 and S60: micropropagated on solid medium in the presence of 30 g/L and 60 g/L NaCl, respectively; L30 and L60: Plants micropropagated in liquid medium in the presence of 30 g/L and 60 g/L NaCl, respectively.

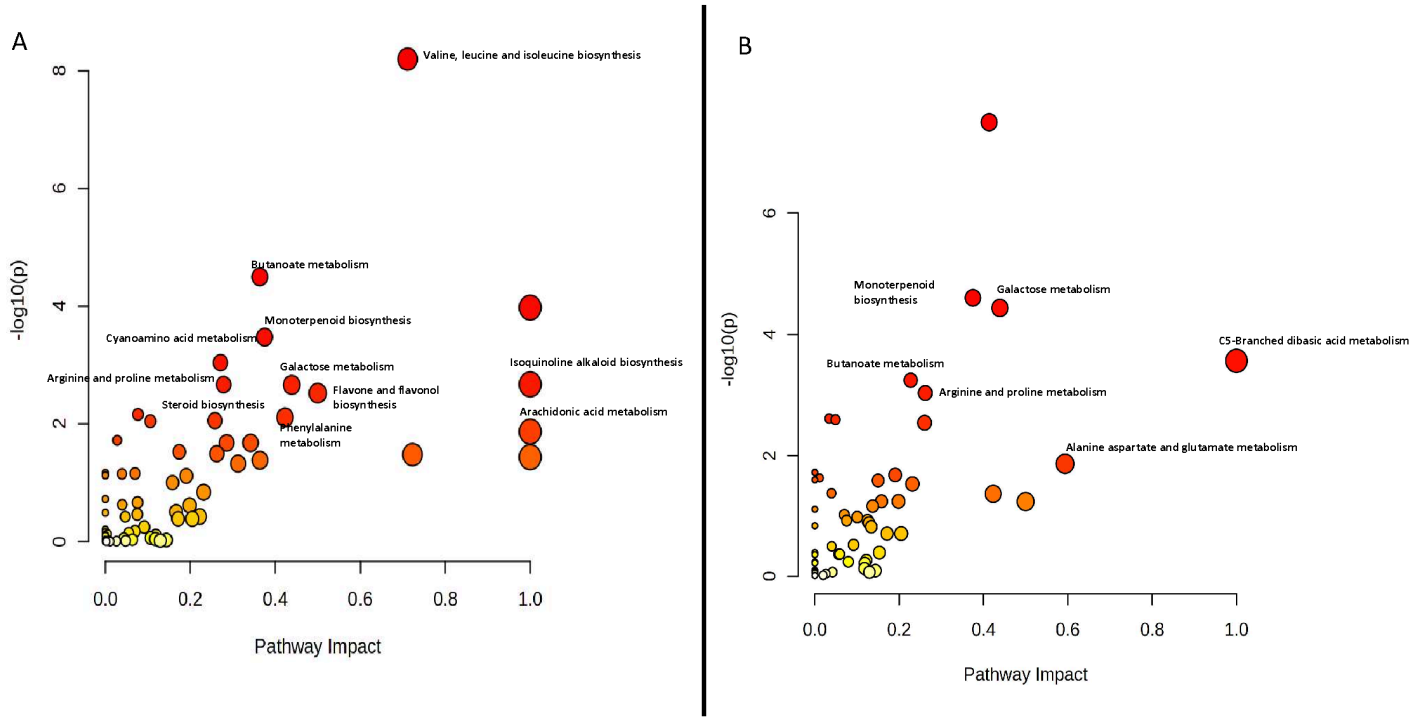


Figure 6

Metabolic pathway analysis using the Mummichog algorithm. Pairwise comparison: A) S30 vs Pooled samples; B) S30 vs S60.

Supplementary Files

This is a list of supplementary files associated with this preprint. Click to download.

- SuplFig2.pdf
- SuplFig1.pdf
- SuplFig3.pdf
- SuplFig6.pdf
- SuplFig5.pdf
- SuplFig4.pdf
- SuplFig8.pdf
- SuplFig7.pdf
- SupplementarymaterialLegends.docx
- SUPPLEMENTARYTABLE1.docx
- SUPPLEMENTARYTABLE3.docx
- SUPPLEMENTARYTABLE4.docx
- SUPPLEMENTARYTABLE2.docx